High-Energy Bremsstrahlung and Electron Pair Production in Thin Crystals

GIORDANO DIAMBRINI PALAZZI
Istituto di Fisica dell' Università di Genova and *Istituto Nazionale di Fisica Nucleare, Genova, Italy*

A survey of theoretical and experimental methods now available for calculating, producing, and measuring high-energy coherent bremsstrahlung (HEB) and electron pair production (EPP) is presented.

After an introduction in which the historical development of the subject matter is sketched, a preliminary theoretical approach is outlined. A rough classical argument is shown, and a formal expression of the Laue–Bragg law suitable for the next calculation is deduced, together with some fundamental kinematics of the HEB and EPP processes. The structure factors for the cubic, face-centered cubic, and diamond lattice are deduced and some qualitative features of the interferential cross sections are shown.

A complete calculation of the HEB and EPP cross sections is carried out. HEB polarized and unpolarized cross sections as functions of recoil momentum are obtained and then integrated over all the reciprocal lattice space. Corresponding results for EPP cross sections are expressed and numerical calculation results are shown.

The last part of the paper deals with experimental methods and techniques used in different laboratories in order to produce and measure high-energy coherent bremsstrahlung suitable for photoproduction experiments by polarized photons. Experimental apparatus and results are described in some detail. Finally, concluding remarks are made concerning the topics omitted.

CONTENTS

I. INTRODUCTION

A. Preface

This paper presents a survey of the high-energy bremsstrahlung and electron pair production in crystals, containing important information on the theoretical basis and experimental methods of calculating, producing, and measuring coherent bremsstrahlung beams from high-energy electron machines.

This survey presents the most (not all) important work on the subject matter from a unified point of view. The next paragraph outlines the chronological development. Some topics are not treated: in this case suitable references are listed. As far as the pioneer work of the Frascati staff is concerned, a survey paper will soon be ready.

B. Historical Background

Perhaps the first idea about these processes may be found in a work of Williams.[1] Ferretti[2] developed semi-qualitative calculations based on the Weizsacker and Williams method of the virtual quanta. Also Ter-Mikaelian and Purcell[3] performed calculations based on the virtual quanta method. The Ter-Mikaelian paper presents a very complete calculation, taking into account the actual structure of the crystal and the temperature effects. Unfortunately this paper has been unknown until now to this author and to the Frascati group, except by title. Feinberg and Pomerranchuk and Dyson and Überall[4] presented other arguments. More recently, Überall[5,6] carried out the full calculation by using the Born approximation and by obtaining results on the cross sections and polarization which could be compared with experiment. These theoretical results stimulated the performance of experiments by means of the high-energy electron accelerators. Some qualitative measurements was carried out by Frisch and Olson[7] at Cornell and by Panofsky and Saxena[8] at Stanford. The first two authors showed an enhancement in the low region of the bremsstrahlung spectrum for a certain crystal orientation. Owing to the poor energy resolution of the measurements, the expected central minimum washed out. The same result was obtained some time later by Saxena.[9]

At the end of 1958 this author developed at Frascati a research program whose final aim was the production of a polarized photon beam useful for experiments in high-energy physics. The experiments at Frascati were

[1] E. J. Williams, Kgl. Danske Videnskab. Selskab., Mat. Fys. Medd. **13**, 4 (1935).
[2] B. Ferretti, Nuovo Cimento **7**, 118 (1950).
[3] M. L. Ter-Mikaelian, Zh. Eksp. Teor. Fiz. **25**, 296 (1953); E. M. Purcell (private communication, 1955).
[4] F. J. Dyson and H. Überall, Phys. Rev. **99**, 604 (1955); E. L. Feinberg and I. Pomeranchuk, Nuovo Cimento Suppl. **3-X**, 652 (1956).
[5] H. Überall, Phys. Rev. **103**, 1055 (1956).
[6] H. Überall, Phys. Rev. **107**, 223 (1957).
[7] O. R. Frisch and D. H. Olson, Phys. Rev. Letters **3**, 141 (1959).
[8] W. K. H. Panofsky and A. N. Saxena, Phys. Rev. Letters **2**, 219 (1959).
[9] A. N. Saxena, Phys. Rev. Letters **4**, 311 (1960).

carried out first by Bologna, Diambrini, and Murtas.[10,11] They showed in both the electron pair production[10] and bremsstrahlung[11] the expected central minimum and only a qualitative agreement with the Überall results, with also systematic differences. A further experimental investigation, carried out with a better angular resolution, showed an unexpected fine structure in the angular dependence of the bremsstrahlung cross sections. It was realized[12,13] that the approximation of continuous lattice planes used in the previous calculations was unsuitable for bremsstrahlung in the giga-electro-volt region, and new calculations were necessary by taking into account the actual structure of the lattice planes.

It was clear that also the bremsstrahlung spectrum would have large peaks with high polarization.[14] Detailed calculations have been carried out.[13,15–18] Barbiellini, Bologna, Diambrini, and Murtas carried out measurements on the coherent-spectrum bremsstrahlung[19] and on the polarization,[20] finding good agreement with the new theoretical results. These authors also proposed a new method for measuring the polarization of very high energy photons by using a second crystal as analyzer.[21] At this point it was clear[22] that coherent bremsstrahlung beams could be obtained also in the multi-giga-electron-volt electron accelerators, without important experimental difficulties. Then this author proposed an experiment at the Desy 6-GeV electron syncrotron in order to get 2–4-GeV polarized photons suitable for experiments. A staff of physicists from Frascati and Desy[23] carried out the experiment successfully, by getting one lattice point photon peak at 2-GeV with 70% polarization. After this they measured[24] the polarization by means of the method proposed by the Frascati group. A group of 10 Japanese researchers of the Tokyo Institute for Nuclear Study measured coherent bremsstrahlung from silicon crystal at the Tokyo 720-MeV electron syncrotron.[25,26] They showed also the effect of the collimation on the width of the peaks, as expected from the paper of De Wire and Mozley.

Finally, we consider the works of Cabibbo, Da Prato, De Franceschi, and Mosco[27,28] concerning the production and the analysis of linearly and circularly polarized high-energy γ rays by using very thick crystals. The conclusions of these authors have not been tested experimentally until now.

II. PRELIMINARY THEORETICAL APPROACH

A. A Classical Argument

The calculation of the coherent bremsstrahlung and electron pair production in crystals has some formal complication. At the end it may be difficult to take up a simple physical interpretation of the classical kind, as it is difficult to gather a flower concealed below a bramble of thorns. However, it is possible to deduce some important feature of the coherent bremsstrahlung by using classical arguments only. As far as the bremsstrahlung intensity is concerned, we shall use a *modified* Frisch[7] argument. Let us consider two nearest parallel rows of atoms of a cubic crystal of lattice spacing a [Fig. 1(a)].

Let a relativistic electron (speed v) move along a direction forming a small angle θ with the rows of atoms. When the electron reaches the atom A (supposed to be a pointlike charge), it will emit an electromagnetic wave train which we suppose to propagate with speed c along the same direction of the electron. When the electron reaches the atom B of the second row, its distance from the beginning of the first wave train will be

$$\Delta l=(c-v)\,(l/v)$$
$$=(1-\beta)l/\beta\approx(1-\beta)l\approx l/2\gamma^2\approx l/2E^2=a/2E^2\theta, \quad (1)$$

where $l=a/\theta$ is the distance A→B and $\gamma=(1-\beta^2)^{-1/2}\approx E$, E being the electron energy in mc^2 units. Therefore, in the new wave train emitted in the interaction of the electron with the atom B, the wave of length λ will have a phase shift $\Delta\varphi=2\pi(\Delta l/\lambda)$. A constructive interference happens when $\Delta\varphi=n2\pi$ (n is an integer number) or $\Delta l=n\lambda$. By using the relation $\lambda=2\pi/K$, where K is the photon momentum (units $\hbar=c=1$), and Eq. (1), we get

$$\Delta l=n\lambda$$

[10] G. Bologna, G. Diambrini Palazzi, and G. P. Murtas, Phys. Rev. Letters **4**, 134 (1960).
[11] G. Bologna, G. Diambrini Palazzi, and G. P. Murtas, Phys. Rev. Letters **4**, 572 (1960).
[12] G. Diambrini Palazzi (unpublished).
[13] G. Diambrini Palazzi, Nuovo Cimento Suppl. **25X**, 88 (1962).
[14] G. Barbiellini, G. Bologna, G. Diambrini Palazzi, and G. P. Murtas, Phys. Rev. Letters **8**, 112 (1962).
[15] G. Barbiellini, G. Bologna, G. Diambrini Palazzi, and G. P. Murtas, Natl. Lab. Frascati Rept. 62/10, February 1962.
[16] G. Barbiellini, Natl. Lab. Frascati Rept. 62/49, June 1962.
[17] G. Bologna, Natl. Lab. Frascati Rept. 62/56, June 1962.
[18] H. Überall, Z. Naturforsch. **17a**, 332 (1962).
[19] G. Barbiellini, G. Bologna, G. Diambrini Palazzi, and G. P. Murtas, Phys. Rev. Letters **8**, 454 (1962).
[20] G. Barbiellini, G. Bologna, G. Diambrini Palazzi, and G. P. Murtas, Phys. Rev. Letters **9**, 396 (1962).
[21] G. Barbiellini, G. Bologna, G. Diambrini Palazzi, and G. P. Murtas, Nuovo Cimento **28**, 436 (1963).
[22] G. Diambrini Palazzi, Proc. Conf. Photon Interactions in the BeV Energy Range, Cambridge, Mass., 1963, p. VI-4.
[23] G. Bologna, G. Lutz, H. D. Schultz, U. Timm, and W. Zimmermann, Nuovo Cimento **42**, 844 (1966).
[24] L. Criegee, G. Lutz, H. D. Schultz, U. Timm, and W. Zimmermann, Nuovo Cimento **16**, 1031 (1966).
[25] S. Kato, T. Kifrne, Y. Kimura, M. Kobayashi, K. Kondo, T. Nishikawa, H. Sasaki, K. Takanratsu, S. Kikuta, and K. Kohra, J. Phys. Soc. Japan **20**, 303 (1965).
[26] T. Kifune, Y. Kimura, M. Kobayashi, and K. Kondo, J. Phys. Soc. Japan **21**, 1905 (1966).
[27] N. Gabibbo, G. Da Prato, G. De Franceschi, and U. Mosco, Nuovo Cimento **27**, 979 (1963).
[28] N. Cabibbo, G. Da Prato, G. De Franceschi, and U. Mosco, Phys. Rev. Letters **9**, 270, 435 (1962).

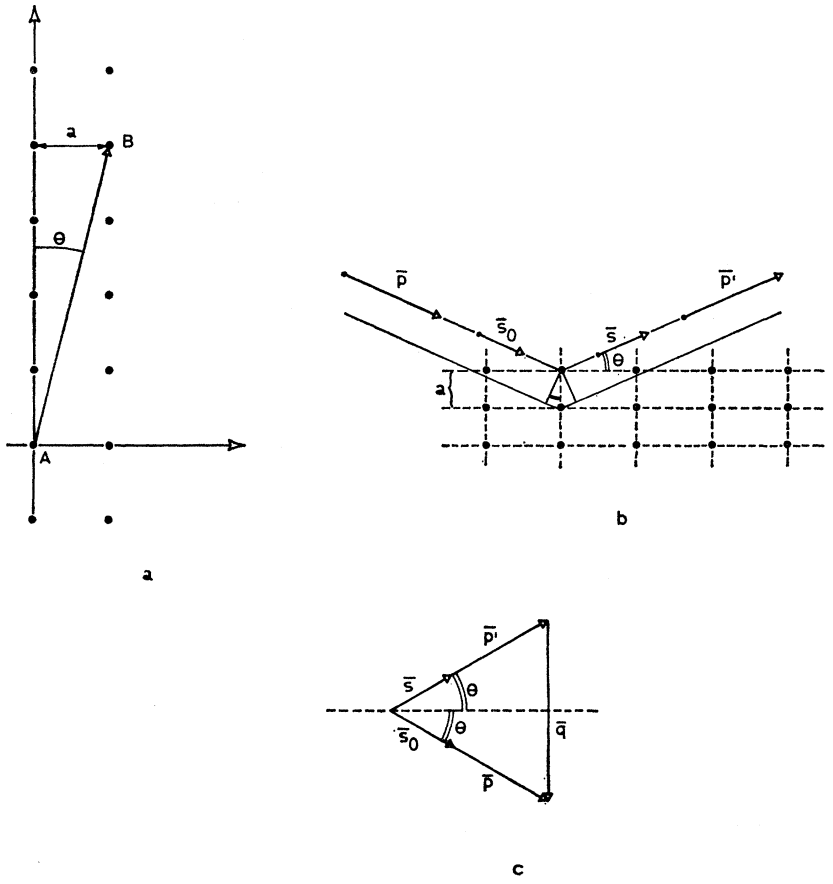

FIG. 1. (a) A→B represents the direction of the incident electron between two parallel rows of atoms in a cubic crystal. (b) **P**, **P'** are the incident and reflected momentum vectors of the incident and reflected particle (or radiation) on the crystal; **S**, $\mathbf{S}_0$ are the respective unitary vectors; $|\mathbf{P}|=|\mathbf{P}'|$. In the figures, overbars denote the vectors used in the text. (c) The recoil momentum $\mathbf{q}=\mathbf{P}-\mathbf{P}'$; $|\mathbf{q}|=2p\sin\theta$.

or

$$a/2E^2\theta=n(2\pi/K)$$

or

$$K/2E^2=n(2\pi/a).$$

Now $E=E_0-K$, if E_0 is the *primary* energy of the electron, and so $K/2E^2=(K/2E_0^2)[1-(K/E_0)]^{-2}$. But the minimum transferred momentum at the nucleus in a bremsstrahlung process is $\delta=K[2E_0^2(1-K/E_0)]^{-1}$; so for $K/E_0\ll 1$ (low-energy photons) we get

$$n(2\pi/a)\theta\approx K/2E_0^2\approx\delta \qquad (K/E_0\ll 1). \qquad (2)$$

As we shall see, the relation $n(2\pi/a)=\delta/\theta$ represents the exact solution. So we have shown that the relation obtained by a simple classical Frisch-like argument gives the right result only when $K/E_0\ll 1$.

B. Physical Meaning and Kinematics

Now let us consider in a cubic crystal the Bragg scattering of a particle beam of momentum **p** before scattering, and **p'** after. We have $|\mathbf{p}|=|\mathbf{p}'|$. The condition for the coherent reflection from the set of planes with spacing a is given by the well-known Bragg condition [see Fig. 1(b)]

$$2a\sin\theta=n\lambda \quad \text{or} \quad 2\sin\theta/\lambda=n/a \qquad (3)$$

by remembering that in this case $\lambda=1/p$ is the De Broglie wave associated to the particles (units in which $h=1$), and we may write

$$2\sin\theta/\lambda=2p\sin\theta=q; \qquad n/a=g,$$

where we mean by q the recoil momentum transferred to the crystal, and by g a vector in the cubic reciprocal lattice of a reciprocal basic vector $1/a$. Thus the Bragg condition (3) may be written now:

$$q=g. \qquad (2')$$

In order to obtain a more general and rigorous derivation of Eq. (2'), we will now start from the phase equation

$$\mathbf{L}\cdot[(\mathbf{s}-\mathbf{s}_0)/\lambda]=hn_1+kn_2+ln_3; \qquad (4)$$

here n_1, n_2, n_3 are a triplet of integer numbers describing the direct lattice, $\mathbf{L}=n_1\mathbf{a}+n_2\mathbf{b}+n_3\mathbf{c}$ is a direct lattice vector, (h, k, l) is the Miller index, and $\mathbf{s}_0$, $\mathbf{s}$ are unit vectors along the incident and reflected directions of the particle beam that interacts with a crystal [see Fig. 1(c)]. We remember the condition $\mathbf{L}\cdot(\mathbf{s}-\mathbf{s}_0)=$ const, and so, for constant λ, $hn_1+kn_2+ln_3=$ const gives the equation of a plane, the so-called reflection plane, perpendicular to the direction of the vector $\mathbf{s}-\mathbf{s}_0$

and placed at a distance $d_{hkl}=[g_{(h,k,l)}]^{-1}$ from the origin, where $g_{(h,k,l)}$ is the reciprocal lattice vector perpendicular to the plane (h, k, l).

Since $\mathbf{L}\cdot(\mathbf{s}-\mathbf{s}_0)$ represents the difference between the path of the beam reflected by this plane and the path of that reflected by the parallel plane through the origin, it follows that $\mathbf{L}\cdot[(\mathbf{s}-\mathbf{s}_0)/\lambda]$ is the phase difference between the beams. But, also, we have [see Fig. 1(c)] $(\mathbf{s}-\mathbf{s}_0)/\lambda=\mathbf{p}-\mathbf{p}'=\mathbf{q}$, where $\mathbf{q}$ is the recoil momentum transferred to the crystal. On the other side we may write

$$hn_1+kn_2+ln_3=(n_1\mathbf{a}+n_2\mathbf{b}+n_3\mathbf{c})\cdot(\mathbf{a}^*h+\mathbf{b}^*k+\mathbf{c}^*l); \tag{4'}$$

here $(\mathbf{a}, \mathbf{b}, \mathbf{c})$ and $(\mathbf{a}^*, \mathbf{b}^*, \mathbf{c}^*)$ are two triplets of basic vectors of the direct and reciprocal lattice, respectively. In fact from the definition of the reciprocal lattice we have the following relations:

$$\mathbf{a}\cdot\mathbf{a}^*=\mathbf{b}\cdot\mathbf{b}^*=\mathbf{c}\cdot\mathbf{c}^*=1;$$

$$\mathbf{a}\cdot\mathbf{b}^*=\mathbf{a}^*\cdot\mathbf{b}=\mathbf{c}\cdot\mathbf{b}^*=\mathbf{c}^*\cdot\mathbf{b}=\mathbf{a}\cdot\mathbf{c}^*=\mathbf{a}^*\cdot\mathbf{c}=0;$$

and with the help of these relations we may obtain (4'). Thus the expression (3) may now be written as

$$\mathbf{L}\cdot\mathbf{q}=\mathbf{L}\cdot\mathbf{g}, \tag{5}$$

where we put the vector $\mathbf{g}=\mathbf{a}^*h+\mathbf{b}^*k+\mathbf{c}^*l$ in a general reciprocal lattice.

Because (5) must be valid for each $\mathbf{L}$ value, the relation follows

$$\mathbf{q}=\mathbf{g}. \tag{6}$$

This relation has a more general physical meaning than (3) or (2'), because in (6) there is no explicit reference to the parameters of the incident beam. Here we have only the transferred momentum to the crystal, whatever the responsible interaction was. So it is possible, of course in principle, to have interference effects for any kind of interaction. But these effects are large enough only if the recoil momentum $\mathbf{q}$ is of the order of the minimum reciprocal lattice vector. Or, in other words, when the wavelength λ_q associated with the recoil q, is of the order of the lattice spacing $\sim a$. This condition is fulfilled in the bremsstrahlung and electron pair production at high energy. In these reactions, in fact, we have $\lambda_q=1/q_p\simeq a_{sc}$, where q_p is the most probable recoil momentum value and a_{sc} is the screening radius of the atom. In the following we explain the way in which the interference phenomena of these two processes may be calculated and understood. Let us consider first the bremssrtahlung process originated by a fast electron (momentum p_1, energy E_1) in the Coulomb field of the nucleus. From momentum conservation, we have the relation $\mathbf{q}=\mathbf{p}_1-\mathbf{p}_2-\mathbf{K}=\mathbf{p}_1-\mathbf{p}'$, where $\mathbf{p}_2$ is the momentum of the electron after the emission of a quantum of momentum $\mathbf{K}$, $\mathbf{q}$ is the recoil momentum of the nucleus, and $\mathbf{p}'$ is the vector $\mathbf{p}_2+\mathbf{K}$ (see Fig. 2).

Let us now suppose that the bremsstrahlung process occurs in a crystal. Then condition (6) imposes certain kinematic conditions that may be derived, for example, by using something like the Ewald construction.

For this we may take the incident and "reflected" vector $\mathbf{p}_1$ and $\mathbf{p}'$, respectively. In Fig. 2 the point 0 represents the origin of the reciprocal lattice, and $\mathbf{g}$ is just a vector of this lattice. For a permitted event of bremsstrahlung the top of the vector $\mathbf{q}$ must coincide with a point of Fig. 2.

Now we look at the distribution of the $\mathbf{q}$ vectors in a semiqualitative way. From the energy and momentum conservation laws we may easily derive the order of magnitude of $q_\perp$ and q_z, the components of $\mathbf{q}$ perpendicular and parallel to the direction of $\mathbf{p}_1$ (see also Ref. 5).

The first important quantity to be determined is the minimum momentum transferred to the nucleus in a bremsstrahlung event. Let us assume that the primary momentum $\mathbf{p}_1$ (and so E_1) of the electron, the energy of the emitted photon K, and the energy E_2 of the scattered electron (momentum p_2) are held constant. The vector $\mathbf{p}'=\mathbf{K}+\mathbf{p}_2$ reaches its maximum value $\mathbf{p}_0$ when $\mathbf{K}$ and $\mathbf{p}_2$ are parallel. In this situation the vector $\mathbf{q}$, for any fixed direction of $\mathbf{p}'$, reaches its minimum value $\mathbf{q}_0=\mathbf{p}_1-\mathbf{p}_0$. The vector $\mathbf{q}_0$ has its extremity on a spherical surface of radius $p_0=p_2+K$, as shown in Fig. 2.

When we also take $\mathbf{p}_0$ parallel to $\mathbf{p}_1$ we may compute the minimum momentum transferred to the nucleus $q_0=\delta$. This is

$$\delta=p_1-p_0=p_1-p_2-K,$$

and by remembering

$$p_{1,2}=(E_{1,2}^2-1)^{1/2}\simeq E_{1,2}(1-\tfrac{1}{2}E_{1,2}^{-2})$$

we obtain

$$\delta=K/2E_1E_2=x/2E_1(1-x),$$

where $x=K/E_1$. This is also the minimum value for q_z. The order of magnitude of the maximum value of q_z is

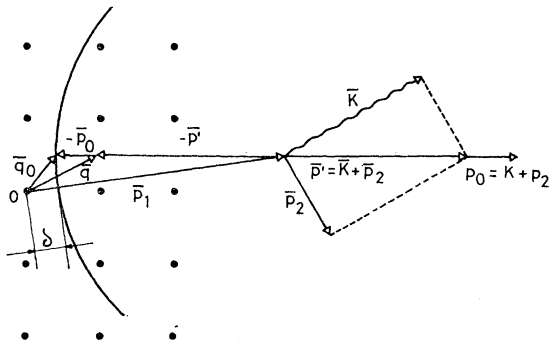

FIG. 2. The Ewald construction for the bremsstrahlung in crystals. 0 is the origin of the reciprocal lattice. $\mathbf{P}_1$ is the incident electron momentum vector; $\mathbf{P}'=\mathbf{K}+\mathbf{P}_2$ is the "reflected" vector; $\mathbf{q}=\mathbf{P}_1-\mathbf{P}'$ is the recoil momentum, which has the minimum value $q_{\min}=\delta=P_1-K-P_2$; and $\mathbf{K}$ and $\mathbf{P}_2$ are the photon and secondary electron momenta.

easily obtained by using for $\theta_1 \sphericalangle(\mathbf{K}, \mathbf{p}_1)$ the value $\theta_1 \approx 1/E_1$, the most probable angle of emission of the photons, and the small-angle approximation, by which we have $\theta_3 = \sphericalangle(\mathbf{p}_2, \mathbf{p}_1) \approx \theta_1 K/E_2 \approx K/E_1E_2$ (Fig. 2). Thus, we have

$$q_z = p_1 - p_2 \cos\theta_3 - K \cos\theta_1 \approx K/E_1E_2 \approx 2\delta.$$

The minimum value of $q_\perp$ is 0; it is also possible to show that the maximum value of $q_\perp$ is about 2 (in our units this means $2mc$).

The results are summarized as follows:

$$\left.\begin{array}{l} \delta \leq q_z \lesssim 2\delta \\ 0 \leq q_\perp \lesssim 2 \end{array}\right\} \qquad \delta = (1/2E_1)[x/(1-x)] \qquad \text{(bremsstr.)}.$$

As far as the electron pair photoproduction is concerned, we may use the same procedure as for the bremsstrahlung, by starting from the momentum conservation equation

$$\mathbf{q} = \mathbf{K} - \mathbf{p}_1 - \mathbf{p}_2,$$

where $\mathbf{K}$ is now the momentum of the incident photon, $\mathbf{p}_1$, $\mathbf{p}_2$ are the momenta of the electron and positron emitted, and $\mathbf{q}$ is the momentum transferred to the nucleus in this process.

Also, for the electron pair production we obtain the results given by (7), where now the minimum transferred momentum is

$$\delta = K/2E_1E_2 = 1/2Ky(1-y),$$

where K, E_1, E_2 are the energies of the incident photon and of the two electrons of the pair, and $y = E_1/K$. In the Table I are reported some typical values of the very important parameter δ. It is seen that the ratio $q_z/q_\perp$ is in the range $10^{-3}-10^{-6}$. So we eventually may conclude that the extremities of the vectors $\mathbf{q}$ from the origin 0 of the reciprocal lattice must lie in a disk-shaped region of thickness δ, perpendicular and coaxial to the $\mathbf{p}_1$ (or $\mathbf{K}$ for the EPP) direction, placed at a distance δ from the origin. Incidentally, the existence of a minimum recoil momentum when all the secondary particles are aligned with the primary beam, gives the possibility of obtaining a kind of interference effect that has no analog in classical Bragg scattering. For the latter, we have $\mathbf{q} = \mathbf{p}_1 - \mathbf{p}' = 0$ [Fig. 1(a)] when the two vectors $\mathbf{p}_1\mathbf{p}'$ are aligned. This is an interesting feature of the high-energy interference effects we are studying. Let us consider again our disk of the momenta in the reciprocal lattice space. If we rotate the crystal each time a reciprocal lattice point enters or leaves the momenta region, the cross section for the process is enhanced or reduced. This variation is important only if the condition $\delta \ll |\mathbf{g}_0| = 2\pi/a$ is fulfilled. In our units (that is, by measuring the lengths in units of $\hbar/mc = 0.024/2\pi$ Å) by taking, for example, a diamond crystal with $a = 3.56$ Å, it will be $2\pi/a = (0.024/3.56)(2\pi/2\pi) = 6.8\times10^{-3} \gg \delta$ for most of the values reported in Table I.

TABLE I. Typical values of δ.

E_1 (GeV)	x	δ Bremss.	K	y	δ Pair prod.
1	0.8	1.02×10^{-3}	1	0.2	1.60×10^{-3}
1	0.3	1.09×10^{-4}	1	0.5	1.02×10^{-3}
6	0.8	1.70×10^{-4}	6	0.2	2.6×10^{-4}
6	0.3	1.8×10^{-5}	6	0.5	1.7×10^{-4}
20	0.8	5.1×10^{-5}	20	0.2	8×10^{-5}
20	0.3	5.4×10^{-6}	20	0.5	5.1×10^{-5}

With an ideal crystal without thermal motion, the recoil is taken by all the crystal and the transferred energy $E_r = q^2/2M_{cr}$ vanishes. The approximation used in the calculation of the cross section of an infinitely heavy nucleus is in this case an exact approximation. We may call it a "recoilless" interaction, using the language of the Mössbauer effect. If we consider an actual crystal with some thermal motion of the atoms always present, only a fraction fN of the N atoms of the crystal does not recoil and does produce interference effects. The remaining part $(1-f)\ N$ of the atoms recoils without any interference effect. The fraction f is given by the factor $f = \exp(-Aq^2)$, where A is the mean-square value of the thermal displacement of the atoms given by

$$A = (3m^2c^2/4MK\Theta)[1+4(T/\Theta)\Gamma(\Theta/T)],$$

where M is the atomic mass, K is the Boltzmann constant, Θ is the Debye temperature of the crystal at the absolute temperature T, and

$$\Gamma\left(\frac{\Theta}{T}\right) = \frac{T}{\Theta}\int_0^{\Theta/T} \frac{t}{e^t-1}\,dt$$

is the Debye function.

C. Structure Factors of Some Crystal Lattices and Qualitative Feature of the Cross Sections

In order to derive the cross section for bremsstrahlung and pair production in a crystal, as shown by Überall,[5] we have to multiply the Debye–Waller diffraction factor by the differential cross section for a single atom expressed as a function of $\mathbf{q}$. We get

$$d\sigma_{cry} = \{|\sum_{\mathbf{L}} \exp(i\mathbf{q}\cdot\mathbf{L})|^2 \exp(-Aq^2) + N[1-\exp(-Aq^2)]\}d\sigma(\mathbf{q}). \quad (7)$$

We showed before the physical meaning of the term $\exp(-Aq^2)$. Now we calculate the Laue–Bragg intensity term $|\sum_{\mathbf{L}} \exp(i\mathbf{q}\cdot\mathbf{L})|^2$ for some simple but very diffuse lattice structures such as simple-cubic (sc), face-centered cubic (fcc), and diamond lattices. The simple-cubic structure is important because it is useful

in order to calculate the other structures. Let us first consider a fundamental cell, parallelepiped, with lattice constants $\mathbf{a}_1$, $\mathbf{a}_2$, $\mathbf{a}_3$ along the three perpendicular axis, and so let $\mathbf{L}=n_1\mathbf{a}_1+n_2\mathbf{a}_2+n_3\mathbf{a}_3$. Let N_1, N_2, N_3, be the number of cells along the directions of $\mathbf{a}_1$, $\mathbf{a}_2$, $\mathbf{a}_3$; thus, by putting

$$\mathbf{q}\cdot\mathbf{a}_1=q_1a_1, \qquad \mathbf{q}\cdot\mathbf{a}_2=q_2a_2, \qquad \mathbf{q}\cdot\mathbf{a}_3=q_3a_3,$$

we have

$$\left|\sum_{n_1,n_2,n_3}\exp(i\mathbf{q}\cdot\mathbf{L})\right|^2=\left|\sum_{n_1=1}^{N_1}\exp(in_1q_1a_1)\right|^2 \times\left|\sum_{n_2=1}^{N_2}\exp(in_2q_2a_2)\right|^2\left|\sum_{n_3=1}^{N_3}\exp(in_3q_3a_3)\right|^2. \quad (8)$$

Now, a short mathematical digression: We have

$$\left|\sum_{n_1=1}^{N_1}\exp(in_1q_1a_1)\right|^2 =\left|\frac{\exp(iN_1q_1a_1)-1}{\exp(iq_1a_1)-1}\right|^2 =\sin^2\tfrac{1}{2}(N_1q_1a_1)/\sin^2\tfrac{1}{2}(q_1a_1); \quad (9)$$

but, because N_1 is a very large number, this is a very peaked function for $q_1a_1/2=h\pi$ ($h=0, 1, 2, \cdots$), and we may write, by introducting the Dirac δ function,

$$\sin^2\tfrac{1}{2}(N_1q_1a_1)/\sin^2\tfrac{1}{2}(q_1a_1)=C\delta[(\tfrac{1}{2}q_1a_1)-h\pi] =(2C/a_1)\delta[q_1-(h2\pi/a_1)]. \quad (10)$$

The normalization constant C is found by integration through the $h=0$ peak:

$$C=\int_{-\pi/2}^{\pi/2}C\delta(\tfrac{1}{2}q_1a_1)\,d(\tfrac{1}{2}q_1a_1) =\int_{-\pi/2}^{\pi/2}\frac{\sin^2 N_1\tfrac{1}{2}(q_1a_1)}{\sin^2\tfrac{1}{2}(q_1a_1)}\,d(\tfrac{1}{2}q_1a_1).$$

By putting $N_1q_1a_1/2=x$, always because N_1 is very large, we obtain

$$C=N_1\int_{-\infty}^{+\infty}\frac{\sin^2 x}{x^2}\,dx=\pi N_1. \quad (11)$$

By substitution of (11) in (10) and of (10) in (9), we get

$$\left|\sum_{n_1=1}^{N_1}\exp(in_1q_1a_1)\right|^2=(2\pi/a_1)N_1\delta[q_1-h(2\pi/a_1)].$$

By substitution in (8) of this result for the three indices, we eventually obtain

$$\left|\sum_{n_1,n_2,n_3}\exp(i\mathbf{q}\cdot\mathbf{L})\right|^2=[(2\pi)^3/a_1a_2a_3]N_1N_2N_3\sum_{h,k,l}\delta[q_1-h(2\pi/a_1)]\delta[q_2-k(2\pi/a_2)]\delta[q_3-l(2\pi/a_3)]$$

$$=[(2\pi)^3/\Delta]N\sum_{h,k,l}\delta(q_1-hb_1')\delta(q_2-kb_2')\delta(q_3-lb_3'), \quad (12)$$

where $\Delta=a_1a_2a_3$ is the volume of the fundamental cell and $N_1N_2N_3$ is the total number of cells in the crystal that may be expressed as a ratio of the number of atoms N in the crystal to the number ν of atoms in the cell. In our case $N_1N_2N_3=N$ because $\nu=1$ (one atom at each corner of the parallelepiped).

The previous expression represents the diffraction factor computed by respect to the main axis of the cell, $\mathbf{a}_1[100]$, $\mathbf{a}_2[010]$, $\mathbf{a}_3[001]$, where $[h, k, l]$ are the Miller indices of the axis (or of the plane perpendicular to this axis). The prime on the b_i' indicates this choice. But we may choose another triplet of axes characterized by the Miller indices h_i, k_i, l_i for $i=1, 2, 3$. In this case we must put

$$b_i=2\pi/d_{hkl}, \quad \text{where} \quad d_{hkl}=\left(\frac{h^2}{a_1^2}+\frac{k^2}{a_2^2}+\frac{l^2}{a_3^2}\right)^{-1/2}$$

is the distance between the plane (hkl) and the origin. If we impose the further restriction $a_1=a_2=a_3=a$ (considered for a cubic cell), we have the more simplified relation

$$d_{hkl}=a/(h^2+k^2+l^2)^{1/2};$$

for example, if we choose the axis [110], [001], [1$\bar{1}$0], we have $b_1=(2\pi/a)\sqrt{2}=b_3$; $b_2=2\pi/a$. Thus, a more general expression of (12) is

$$\left|\sum_{n_1,n_2,n_3}\exp(i\mathbf{q}\cdot\mathbf{L})\right|^2=[(2\pi)^3/\Delta]N\sum_{g_1,g_2,g_3}\delta(q_1-g_1)\delta(q_2-g_2)\delta(q_3-g_3), \quad (13)$$

where $g_1=h_1b_1$, $g_2=h_2b_2$, $g_3=h_3b_3$, and h_1, h_2, h_3 is a new triplet of integers.

Now let us calculate the Laue–Bragg term (8) for a face-centered cubic (fcc) lattice. Such a lattice may be obtained by summing up four simple cubic lattices, three of which are translated with respect to one-fourth of the

quantities $(\frac{1}{2}, \frac{1}{2}, 0)$, $(0, \frac{1}{2}, \frac{1}{2})$, $(\frac{1}{2}, 0, \frac{1}{2})$. By writing $\mathbf{L}=a(n_1\mathbf{i}+n_2\mathbf{j}+n_3\mathbf{k})$ (with $\mathbf{i}$, $\mathbf{j}$, $\mathbf{k}$ versors), we have

$$F_{\text{fcc}}=\sum_{\text{fcc}}\exp(i\mathbf{q}\cdot\mathbf{L})=\sum_{\text{sc}}\exp(i\mathbf{q}\cdot\mathbf{L})+\sum_{\text{sc}}\exp\{i\mathbf{q}\cdot[\mathbf{L}+\tfrac{1}{2}a(\mathbf{i}+\mathbf{j})]\}$$
$$+\sum_{\text{sc}}\exp\{i\mathbf{q}\cdot[\mathbf{L}+\tfrac{1}{2}a(\mathbf{j}+\mathbf{k})]\}+\sum_{\text{sc}}\exp\{i\mathbf{q}\cdot[\mathbf{L}+\tfrac{1}{2}a(\mathbf{i}+\mathbf{k})]\}$$
$$=\sum_{\text{sc}}\exp(i\mathbf{q}\cdot\mathbf{L})\{1+\sum\exp[i\mathbf{q}\cdot\tfrac{1}{2}a(\mathbf{i}+\mathbf{j})]+\sum\exp[i\mathbf{q}\cdot\tfrac{1}{2}a(\mathbf{j}+\mathbf{k})]+\sum\exp[i\mathbf{q}\cdot\tfrac{1}{2}a(\mathbf{i}+\mathbf{k})]\}. \quad (14)$$

We know that the reciprocal lattice of a simple cubic lattice of side a is again a cube of side $2\pi/a$. So, the condition $\mathbf{q}=\mathbf{g}$ gives $\mathbf{q}=(h2\pi\mathbf{i}/a)+(k2\pi\mathbf{j}/a)+(l2\pi\mathbf{k}/a)$. By substitution in (14) we obtain

$$F_{\text{fcc}}=[\sum_{\text{sc}}\exp(i\mathbf{q}\cdot\mathbf{L})]\{1+\exp[i2\pi\tfrac{1}{2}(h+k)]+\exp[i2\pi\tfrac{1}{2}(k+l)]+\exp[i2\pi\tfrac{1}{2}(h+l)]\}. \quad (15)$$

The second factor may be called the structure factor of the face-centered cubic lattice. The expression $|\sum_{\text{sc}}\exp(i\mathbf{q}\cdot\mathbf{L})|^2$ is given by (12) or, if we choose an arbitrary triplet of axes, by (13), and in this case instead of (h, k, l) we have another triplet of integers (h_1, h_2, h_3).

The structure factor of the diamond lattice may be obtained by summing up two fcc lattices displaced along the diagonal by $(\frac{1}{4}, \frac{1}{4}, \frac{1}{4})$. Thus, we have for the displaced cube

$$F_{\text{fcc}}'=\sum_{\text{fcc}}\exp\{i\mathbf{q}\cdot[\mathbf{L}+\tfrac{1}{4}a(\mathbf{i}+\mathbf{j}+\mathbf{k})]\}=[\sum_{\text{fcc}}\exp(i\mathbf{q}\cdot\mathbf{L})]\exp[i\mathbf{q}\cdot\tfrac{1}{4}a(\mathbf{i}+\mathbf{j}+\mathbf{k})]=F_{\text{fcc}}\exp[i(\pi/2)(h+k+l)],$$

and for the diamond lattice

$$F_{\text{dia}}=F_{\text{fcc}}+F_{\text{fcc}}'=F_{\text{fcc}}\{1+\exp[i(\pi/2)(h+k+l)]\}.$$

By remembering (13) and (15) and by supposing an arbitrary choice of the reference axes, we obtain for the intensity factor for the diamond

$$|\sum_{\text{dia}}\exp(i\mathbf{q}\cdot\mathbf{L})|^2=[(2\pi)^3/\Delta]\tfrac{1}{8}N|S|^2\sum_{g_1,g_2,g_3}\delta(q_1-g_1)\delta(q_2-g_2)\delta(q_3-g_3),$$

with

$$S=\{1+\exp[i2\pi\tfrac{1}{2}(h_1+h_2)]+\exp[i2\pi\tfrac{1}{2}(h_2+h_3)]+\exp[i2\pi\tfrac{1}{2}(h_1+h_3)]\}\{1+\exp[i(\pi/2)(h_1+h_2+h_3)]\}. \quad (16)$$

We call $|S|^2$ the structure factor of the diamond lattice. This factor diminishes or increases the contributions from some points (or reflections) of a simple cubic lattice. Now we have $\nu=8$ atoms in the fundamental diamond cell.

There is evidence from (13) that the interference part of the cross section increases when the volume Δ decreases with respect to the incoherent part. For example, the ratio $\Delta_{\text{si}}/\Delta_{\text{dia}}$ for silicon and diamond crystals is about 3. It is also important that the thermal motion amplitude A be as small as possible, or the Debye temperature Θ as large as possible. For diamond, $\Theta=1870°\text{K}$, $A=126$; and for silicon, $\Theta=645°\text{K}$, $A=282$, all values at room temperature ($T=293°\text{K}$). Thus a diamond crystal shows a larger interference cross section than a silicon crystal.

In order to derive the semiqualitative features of the interference effect we may choose a certain crystal lattice and then calculate, using (16), the reciprocal lattice and eventually represent in this space the recoil momentum vectors.

Let us choose a diamond lattice. Now the following case is considered. Let the primary electron (or photon) momentum $\mathbf{p}_1$ (or $\mathbf{K}$) make a small angle θ with the axis $[110]=\mathbf{b}_1$. Thus, we are interested in knowing the first reciprocal lattice planes normal to this axis. In fact, the main experimental measurements used this orientation in order to obtain larger-spaced reciprocal lattice points. As in the previous example, for the axis [110], [001], $[1\bar{1}0]$, the spacing is $b_1=b_2=(2\pi/a)\sqrt{2}$, $b_3=2\pi/a$.

Thus, we obtain the reciprocal lattice plane [001], $[1\bar{1}0]$ through the origin (000) ($h_1=0$) and through the (110) point ($h_1=1$) by using in the structure factor (16) the triplets of integer numbers:

			$[001]=\vec{b}_3\uparrow$			
			⋯ 003	⋯	⋯	⋯
			⋯ 002	$1\bar{1}2$	$2\bar{2}2$	$3\bar{3}2$
⋯	⋯	⋯	001	$1\bar{1}1$	$2\bar{2}1$	$3\bar{3}1$
$\bar{3}30$	$\bar{2}20$	$\bar{1}10$	000	$1\bar{1}0$	$2\bar{2}0$	$3\bar{3}0\longrightarrow$
						$[1\bar{1}0]=\vec{b}_2$
⋯	⋯	⋯	$00\bar{1}$	⋯	⋯	⋯
			002	⋯	⋯	⋯

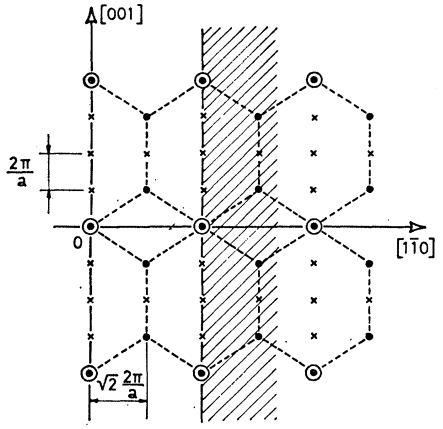

FIG. 3. The reciprocal lattice plane through $h_1=0$ for the diamond crystal (see text).

In this way we obtain the reciprocal lattice planes of Figs. 3 and 4. For the next parallel plane through the point (110) of the [110] axis

$$\begin{array}{cccc} \uparrow[001] & & & \\ 113 & 203 & 3\bar{1}3 & 4\bar{2}3 \\ 112 & 202 & 3\bar{1}2 & 4\bar{2}2 \\ 111 & 201 & 3\bar{1}1 & 4\bar{2}1 \\ & & & [1\bar{1}0] \\ 110 & 200 & 3\bar{1}0 & 4\bar{2}0\longrightarrow \end{array} .$$

For the points enclosed in circles (in Figs. 3 and 4) $|S|^2=64$; for the other points $|S|^2=32$; for the crosses $|S|^2=0$.

The structure of the plane through the point $h_1=1$ (Fig. 4) is the same of that through the point $h_1=0$, but the origin is deplaced. The planes through $h_1=0$, 2, 4, $\cdots$, $2n$ have the same structure, and also the planes through $h_1=1$, 3, 5, $\cdots$, $2n+1$.

In Fig. 5 the whole tridimensional reciprocal lattice is shown. If we assume that the recoil momenta of the nuclei are applied to the origin, the extremities of the

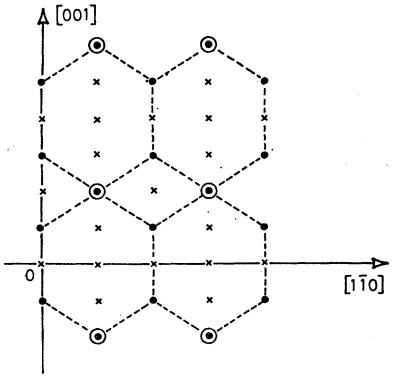

FIG. 4. The reciprocal lattice plane through $h_1=1$ for the diamond crystal (see text).

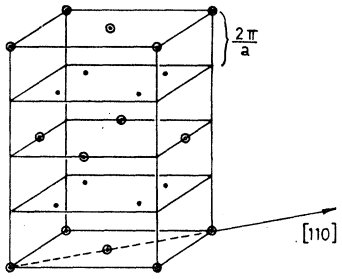

FIG. 5. The reciprocal lattice for a diamond crystal.

nuclei belong to a region whose intersection with the drawing plane is the dashed region in Fig. 6.

The boundary line is at a distance about δ from the origin, as may be seen in Fig. 6. Let us consider the bremsstrahlung case. If we fix the angle θ when the photon energy $x=K/E_1$ increases, the boundary of Fig. 6 moves to the right, because $\delta=x/2E_1(1-x)$ also increases.

Each time the boundary crosses a row of points, a peak in the intensity of the bremsstrahlung spectrum arises at the x value, which satisfies the condition $\delta=\theta h_2\sqrt{2}(2\pi/a)$. If the photon energy (momentum $\delta=\delta_0$) is fixed and the angle θ is changed, some intensity peak arises at values given by $\theta=\delta_0 a/(h_2 2\pi\sqrt{2})$. If we take a typical value from Table I, for example, $\delta=10^{-4}$ (the case where $E_1=1$ GeV, $x\approx 0.3$, diamond crystal) we get the values

$$\theta=10^{-4}/h_2 6.8\times 10^{-3}\times 1.41\approx 10^{-2}/h_2 \text{ rad},$$

with $h_2=1$, 2, 3, $\cdots$. Thus, only small values of θ are involved. The small-angle approximation is used in all of the following calculations.

III. CALCULATION OF THE BREMSSTRAHLUNG AND ELECTRON PAIR PRODUCTION CROSS SECTIONS IN THIN CRYSTALS

A. Bremsstrahlung

This section contains a survey of the calculations of cross sections. We follow a line of calculation a little

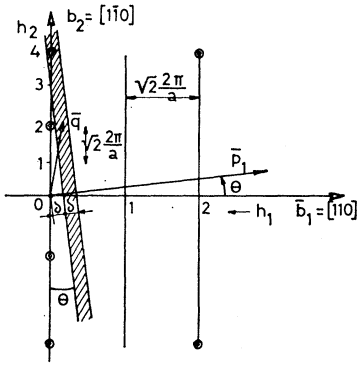

FIG. 6. The reciprocal lattice in the incidence plane, with the intersection of the recoil momentum space.

[29] M. May, Phys. Rev. 84, 265 (1951).

different from that of the Überall paper. We have seen that the crystal allows only those processes in which the recoil momentum has some definite value equal to the vectors of the reciprocal lattice ($\mathbf{q}_i=\mathbf{g}_i$). We begin from the bremsstrahlung and compute the cross section $d\sigma$ for the total intensity for a single atom as a function of $\mathbf{q}$ and compute the polarization of the γ-ray beam by reference to the plane ($\mathbf{p}_1$, $\mathbf{q}$) determined by the directions of the incident electron and of the recoil momentum. After this we are ready to sum up the cross sections over all the points of the reciprocal lattice in order to obtain the coherent part of the cross section, finally adding the incoherent part.

We start from the differential cross section for bremsstrahlung, linearly polarized, that has been computed by May[29] using the Born, small-angle, and high-energy approximations. This expression is the cross section for production of a photon of momentum $\mathbf{K}$ at a fixed direction, with the polarization $\boldsymbol{\varepsilon}$ and the momentum $\mathbf{p}_2$ of the scattered electron at fixed directions. The May[29] cross section, by neglecting a second-order q^2 term, is

$$d^5\sigma_M=(\sigma_0/\pi^2)F(q^2)(E_2/KE_1)4E_1^2E_2^2dK\theta_1d\theta_1\theta_2d\theta_2d\phi_1d\phi_2\{(A\cos\omega+B\sin\omega)^2+C\}, \tag{17}$$

where, in May's notation, the coefficients A, B, C, are defined by the following expressions:

$$A=[E_2\theta_2\cos\varphi/(1+\theta_2^2E_2^2)]-[\theta_1E_1/(1+\theta_1^2E_1^2)];$$

$$B=E_2\theta_2\sin\phi/(1+\theta_2^2E_2^2);$$

$$C=K\delta[(\theta_1^2E_1^2+\theta_2^2E_2^2-2\theta_1\theta_2E_1E_2\cos\phi)/2(1+\theta_1^2E_1^2)(1+\theta_2^2E_2^2)];$$

and

$$\sigma_0=(Z^2/137)(e^2/mc^2)^2=0.5794\times10^{-27}Z^2\ \text{cm}^2,$$

$$F(q^2)=\text{atomic form factor},$$

$$\delta=K/2E_1E_2=\text{minimum recoil momentum of the nucleus}.$$

The variables used in these relations are (Fig. 7) E_1, $\mathbf{p}_1$; E_2, $\mathbf{p}_2$; K, $\mathbf{K}$: energy and momentum of the primary electron, of the scattered electron, and of the emitted photon. $\mathbf{q}=\mathbf{p}_1-\mathbf{p}_2-\mathbf{K}$: recoil momentum of the nucleus. $\theta_1=\sphericalangle\,\mathbf{p}_1\mathbf{K}$; $\theta_2=\sphericalangle\,\mathbf{p}_2\mathbf{K}$: angles of the primary and scattered electrons with respect to the photon direction. $\phi_1=\sphericalangle\,(\mathbf{p}_1,\mathbf{K})(\mathbf{b}_1,\mathbf{K})$; $\phi_2=\sphericalangle\,(\mathbf{p}_2,\mathbf{K})(\mathbf{b}_1,\mathbf{K})$: azimuth of the plans of the primary and scattered electrons (through the $\mathbf{K}$ direction) with respect to the ($\mathbf{b}_1$, $\mathbf{K}$) plane, where $\mathbf{b}_1$ is an arbitrary fixed vector. $\phi=\phi_2-\phi_1=\sphericalangle\,(\mathbf{p}_2,\mathbf{K})(\mathbf{p}_1,\mathbf{K})$: angle between the planes (through $\mathbf{K}$) of the primary and scattered electrons directions. $\omega=\sphericalangle\,(\mathbf{p}_1,\mathbf{K})(\boldsymbol{\varepsilon},\mathbf{K})$: angle between the planes of the primary electron and polarization (always through $\mathbf{K}$).

It is important to measure the angle with reference to the direction of the incident electron for experimental reasons. In fact we have to use the well-collimated electron beam of a high-energy accelerator by integrating over the emission angle of the photons.

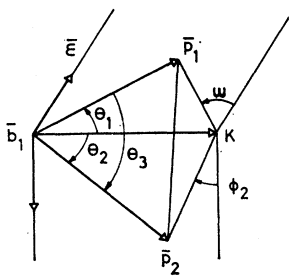

FIG. 7. Graphic sketch for angle definitions in the bremsstrahlung process (see text).

As the next step, we express the cross section through the three components of $\mathbf{q}$ or equivalent variables. Also, we want to refer the polarization plane ($\boldsymbol{\varepsilon}$, $\mathbf{p}_1$) to the plane ($\mathbf{q}$, $\mathbf{p}_1$). For these changes, we use a new set of angles (see also Fig. 8):

$$\theta_3=\sphericalangle\,\mathbf{p}_1,\mathbf{p}_2;$$

$$\theta_1=\sphericalangle\,\mathbf{K},\mathbf{p}_1;$$

$$\theta_2=\sphericalangle\,\mathbf{p}_2,\mathbf{K};$$

$$\psi_1=\sphericalangle\,(\mathbf{K},\mathbf{p}_1)(\mathbf{b}_1,\mathbf{p}_1);$$

$$\psi_3=\sphericalangle\,(\mathbf{p}_2,\mathbf{p}_1)(\mathbf{b}_1,\mathbf{p}_1);$$

$$\psi=\psi_3-\psi_1=\sphericalangle\,(\mathbf{p}_2,\mathbf{p}_1)(\mathbf{K},\mathbf{p}_1);$$

$$\omega'=\sphericalangle\,(\mathbf{p}_1,\mathbf{K})(\boldsymbol{\varepsilon},\mathbf{p}_1);$$

$$\gamma=\sphericalangle\,(\mathbf{q},\mathbf{p}_1)(\mathbf{K},\mathbf{p}_1);$$

$$\varphi=\psi_1+\gamma=\sphericalangle\,(\mathbf{q},\mathbf{p}_1)(\mathbf{b}_1,\mathbf{p}_1).$$

In a good approximation we may take $\omega=\omega'$. In fact the cosine of the angle between two unitary vectors $\mathbf{n}_1$, $\mathbf{n}_2$ normal, respectively, to the planes ($\boldsymbol{\varepsilon}$, $\mathbf{p}_1$) and ($\boldsymbol{\varepsilon}$, $\mathbf{K}$) is given by

$$\cos(\mathbf{n}_1,\mathbf{n}_2)=[(\hat{\varepsilon}\times\hat{p}_1)\cdot(\hat{\varepsilon}\times\hat{K})]/|\,\hat{\varepsilon}\times\hat{p}_1\,|, \tag{18}$$

where $\hat{\varepsilon}$, $\hat{p}_1$, $\hat{K}$ are unit vectors along the directions of $\boldsymbol{\varepsilon}$, $\mathbf{p}_1$, $\mathbf{K}$.

By reference to Cartesian axes x, y, z, by taking the axis z along $\mathbf{p}_1$, and by taking in account $\boldsymbol{\varepsilon}\perp\mathbf{K}$, we may

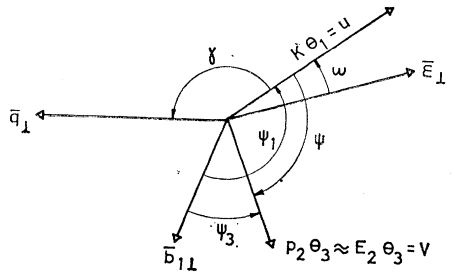

FIG. 8. Graphic sketch for angle definitions in the bremsstrahlung process. The plane of the drawing is perpendicular to the $\mathbf{p}_1$ direction (momentum of the incident electron, see text).

obtain from (18)

$$\cos(\mathbf{n}_1, \mathbf{n}_2) = \cos\theta_1/(1-\epsilon_z^2)^{1/2} \approx (1-\tfrac{1}{2}\theta_1^2)/(1-\theta_1^2)^{1/2} \approx 1,$$

because $\theta_1^2 \approx \epsilon_z^2 \approx 1/E_1^2$.

The first step is the change of the variables $\theta_2 \to \theta_3$, $\phi \to \psi$ that operate the transformation from the May cross section (17) to the following new expression, in which all the angles have reference to the $\mathbf{p}_1$ direction:

$$d^5\sigma_b = (\sigma_0/\pi^2)F(q^2)(E_2/KE_1)4E_1^2E_2^2 dK\theta_1 d\theta_1\theta_3 d\theta_3 d\psi_1 d\psi_3 \times\{(A'\cos\omega + B'\sin\omega)^2 + C'\}. \quad (19)$$

We may obtain the new coefficient A', B', C' by using the relations

$$\theta_2^2 = \theta_1^2 + \theta_3^2 - 2\theta_1\theta_3\cos\psi,$$

$$\theta_2\cos\phi = \theta_1 - \theta_3\cos\psi,$$

$$\theta_2\sin\phi = \theta_3\sin\psi.$$

These coefficients are

$$A' = -\frac{E_1\theta_1}{1+E_1^2\theta_1^2} + \frac{E_2(\theta_1 - \theta_3\cos\psi)}{D},$$

$$B' = \frac{E_2\theta_3\sin\psi}{D},$$

$$C' = K\delta\frac{K^2\theta_1^2 + E_2^2\theta_3^2 + 2KE_2\theta_1\theta_3\cos\psi}{2(1+E_1^2\theta_1^2)D},$$

where

$$D = 1 + E_2^2\theta_1^2 + \theta_3^2E_2^2 - 2E_2^2\theta_3\theta_1\cos\psi = 1 + E_2^2 \times(\theta_1^2 + \theta_3^2 - 2\theta_3\theta_1\cos\psi).$$

The second step consists in changing the variables again in order to obtain for (19) an expression as a function of θ_1 and of the three components of $\mathbf{q}$ or three other variables directly depending on those. It is convenient to use the quantities θ_1^2, q_z, $q_\perp^2$, φ, where q_z, $q_\perp$ are the components of $\mathbf{q}$ parallel or perpendicular to the $\mathbf{p}_1$ direction and φ is the azimuth angle defined as before.

Thus, for this aim we must make the change

$$(\theta_1, \theta_3, \psi_1, \psi_3) \to (u^2, q_z, q_\perp^2, \varphi).$$

It is convenient to put $u = K\theta_1$, $v = E_2\theta_3$, and to use the relations[5]

$$v^2 = 2E_2(q_z - \delta) - (E_2u^2/K),$$

$$uv\cos\psi = \tfrac{1}{2}(q_\perp^2 - u^2 - v^2) = \tfrac{1}{2}\{q_\perp^2 - 2E_2(q_z - \delta) + [(E_2-1)/K]u^2\}. \quad (20)$$

For substitution of the differential factor we have to use the Jacobian

$$J = |\partial(\theta_1, \theta_3, \psi_1, \psi_3)/\partial(u^2, q_z, q_\perp^2, \varphi)| = (4Ku^2v^2\sin\psi)^{-1} = [2Kuv(au^4 + bu^2 + c)^{1/2}]^{-1},$$

where $a = (E_1^2/K^2)$; $b = 2[(\epsilon/\delta) + (q_\perp^2 - 1)]$; $c = 2E_2(\eta - \delta)$; $\eta = q_z - (q_\perp^2/2E_2)$; $\epsilon = q_z - (q_\perp^2/2E_1)$.

After these substitutions we obtain from (19) the expression

$$d^5\sigma_b = (\sigma_0/4\pi)F(q^2)[16E_1^2E_2^2/2K^3E_1(au^4 + bu^2 + c)^{1/2}][(A''\cos\omega + B''\sin\omega)^2 + C'']dKdu^2dq_zdq_\perp^2d\varphi, \quad (21)$$

where A'', B'', C'' are functions of the new variable. But this is always the cross section for bremsstrahlung of a photon with the polarization vector $\boldsymbol{\varepsilon}$ making an angle ω with the emission plane $(\mathbf{K}, \mathbf{p}_1)$.

Instead we want to obtain the two cross sections for emission of a photon with the polarization vector parallel and perpendicular to the plane $(\mathbf{q}, \mathbf{p}_1)$.

From Fig. 2 we see that we may take $\omega = -\gamma$ (thus, $\cos\omega = \cos\gamma$, $\sin\omega = -\sin\gamma$) for $d^5\sigma_{||}$ and $\omega = \frac{1}{2}\pi\gamma$ (thus, $\cos\omega = \sin\gamma$, $\sin\omega = \cos\gamma$) for $d^5\sigma_\perp$. After substitution in (21) we may eliminate $\sin\gamma$, $\cos\gamma$ by the relations

$$\sin\gamma = (v/q_\perp)\sin\psi; \qquad \cos\gamma = (u + v\cos\psi)/q_\perp;$$

and again by the relations (20).

Eventually we obtain

$$d^5\sigma_{||}(\mathbf{q},\mathbf{p}_1)=\frac{\sigma_0}{4\pi}\frac{1}{2E_1K^3}F(q^2)\,(au^4+bu^2+c)^{-1/2}\left\{\frac{E_1^2}{q_\perp^2\delta^2}\left[\frac{\delta}{\epsilon}\left(\frac{u^2E_1}{K}-q_\perp^2\frac{K-E_2}{K}-2E_2(q_z-\delta)\right)\right.\right.$$

$$\left.\left.-\frac{K^2}{K^2+E_1^2u^2}\left(u^2\frac{E_1}{K}+q_\perp^2-2E_2(q_z-\delta)\right)\right]^2+\frac{4E_1E_2K^4\delta q_\perp^2}{(K^2+E_1^2u^2)\epsilon}\right\}dKdu^2dq_zdq_\perp^2d\varphi, \tag{22a}$$

$$d^5\sigma_\perp(\mathbf{q},\mathbf{p}_1)=(\sigma_0/4\pi)F(q^2)\,(2K^3E_1)^{-1}(au^4+bu^2+c)^{-1/2}$$

$$\times\left\{\frac{E_1^2}{\delta^2q_\perp^2}\left(\frac{\delta}{\epsilon}-\frac{K^2}{K^2+E_1^2u^2}\right)^2(au^4+bu^2+c)+\frac{4E_1E_2K^4\delta q_\perp^2}{(K^2+E_1^2u^2)\epsilon}\right\}dKdu^2dq_zdq_\perp^2d\varphi. \tag{22b}$$

These formulas are cross sections for emission of a photon with its polarization vector parallel or perpendicular to the plane $(\mathbf{q},\mathbf{p}_1)$ at the angle $\theta_1=u/K$. But for experimental reasons we need an integration over the angle θ_1 or u^2. It is convenient to obtain the integrations

$$d^4\sigma_b=\int_{u^2}(d^5\sigma_{||}+d^5\sigma_\perp),$$

$$P_qd^4\sigma_b=\int_{u^2}(d^5\sigma_\perp-d^5\sigma_{||}), \tag{23}$$

where $P_q=[(d^4\sigma_\perp-d^4\sigma_{||})/(d^4\sigma_\perp+d^4\sigma_{||})]_{(\mathbf{q},\,\mathbf{p}_1)}$ is the polarization of the whole bremsstrahlung cone related to the plane through the recoil momentum of the nucleus and the incident electron direction. It would be possible to derive the first of (23) directly from the differential Bethe and Heitler cross section, as Überall did in his paper.[5] It is possible to integrate (23) analytically by appropriate change of variable. The results are

$$Kd^4\sigma_b=K(d^4\sigma_{||}+d^4\sigma_\perp)=\frac{\sigma_0}{2\pi}F(q^2)\,\frac{K}{E_1^2}\left\{-\frac{1}{\epsilon^2}+\frac{(1+\epsilon\delta)q_\perp^2+2}{\epsilon(\eta^2+4\delta^2q_\perp^2)^{1/2}}-\frac{\epsilon+\delta q_\perp^2}{[(\eta^2+4\delta^2q_\perp^2)^3]^{1/2}}\right\}dq_zdq_\perp^2d\varphi dK$$

$$\approx\sigma_0\{[1+(1-x)^2]F_1-\tfrac{2}{3}(1-x)F_2\}dq_zdq_\perp^2d\varphi dK, \tag{24a}$$

$$K(d^4\sigma_\perp-d^4\sigma_{||})=\frac{\sigma_0}{2\pi}F(q^2)\,\frac{E_2}{\delta E_1}\left\{3\left[\frac{\eta}{(\eta^2+4\delta^2q_\perp^2)^{1/2}}-1\right]+\frac{4\delta^2q_\perp^2}{\epsilon(\eta^2+4\delta^2q_\perp^2)^{1/2}}+\frac{2\delta^2q_\perp^2(\epsilon+\delta q_\perp^2)}{[(\eta^2+4\delta^2q_\perp^2)^3]^{1/2}}\right\}dq_zdq_\perp^2d\varphi dK$$

$$\approx\sigma_0 2(1-x)F_3dq_zdq_\perp^2d\varphi dK, \tag{24b}$$

where

$$x=K/E_1;$$

$$F_1=(2\pi)^{-1}F(q^2)\,(\delta q_\perp^2/q_z^2);$$

$$F_2=\{6\delta^2q_\perp^2(q_z-\delta)/2\pi[F(q^2)]^{-1}q_z^4\};$$

$$F_3=-[\delta^3q_\perp^2F(q^2)/2\pi q_z^4]=-F_1(\delta^2/q_z^2).$$

Thus, we may derive the interesting value

$$P_q=[(d^4\sigma_\perp-d^4\sigma_{||})/(d^4\sigma_\perp+d^4\sigma_{||})]$$

$$=-2(1-x)F_3/\{[1+(1-x)^2]F_1-\tfrac{2}{3}(1-x)F_2\}$$

$$=-\frac{2(1-x)\delta^2/q_z^2}{[1+(1-x)^2]-4(1-x)\,(\delta/q_z^2)\,(q_z-\delta)}. \tag{25}$$

This expression represents the polarization of photons with fractional energy x, emitted when the recoil momentum of the nucleus has components q_z, $q_\perp$. Since the polarization is computed with respect to the plane $(\mathbf{q},\mathbf{p}_1)$, the angle φ does not appear. The photons are polarized in this plane because of the minus sign in (25). It is easily seen that for $x\approx0$ (very low energy photons) we have $0.5\leq-P_q\leq1$ for $\delta\leq q_z\leq2\delta$.

Now let us consider the case of the bremsstrahlung in a crystal. We may choose a certain crystal orientation by which the intersection of the pancake surface with the plane through $(h=0)$ passes through only a point of the reciprocal lattice. This is actually possible.[23] In this case we have $q_{zi}=\delta$ and (25) becomes simply

$$P_{qi}=-[2(1-x)/1+(1-x)^2]\underset{x\to0}{\longrightarrow}1. \tag{26}$$

This is the polarization value with respect to the plane $(\mathbf{p}_1,\mathbf{q})$, when we take in account only a point of the reciprocal lattice and the coherent part of the cross section only just at the peak $(q_z=\delta)$ of the brems-

strahlung intensity. A surprising property of (26) is its independence from all the parameters except x. This means that, under the limitations listed above, this polarization value is independent of the crystal structure, of the $|\mathbf{q}| = |\mathbf{g}|$ value chosen, of the atomic number Z, and of the crystal temperature.

The total number of photons $N_\perp + N_{||}$ is different, but not the P_{qi} value given in (26). Also, if we obtain the contribution of only a point of the reciprocal lattice, as far as the experimental conditions are concerned, we have always a contribution of the incoherent and unpolarized part of the cross section which depends on the above parameters. In any case it is important to know that the expression (26) represents the theoretical maximum value available for the polarization of the bremsstrahlung in crystals.

Now we proceed to calculate the general and complete expressions for the intensity and polarization in crystals.

As we have seen in Sec. II.C, Überall has shown that the condition $\mathbf{q}=\mathbf{g}_i$, the thermal effect, and the weight of the contribution to the bremsstrahlung or pair production from each single point $\mathbf{g}$ of the reciprocal lattice may be taken into account by using the diffraction factor and integration over the all $\mathbf{q}$ values, for all $\mathbf{g}$ values. So, by putting the expressions (24a), (24b) into Eq. (7) we obtain for the intensity and polarization of the bremsstrahlung,

$$d\sigma_{\text{cry}} = (\sigma_0/K)(2\pi/a)^3 N_1N_2N_3 \sum_{\mathbf{g}} |S|^2 \int_{\mathbf{q}} \delta(\mathbf{q}-\mathbf{g}) \exp(-Aq^2)\sigma(\mathbf{q})\, dq_\perp^2 dq_z d\varphi dK$$

$$+N\int_{\mathbf{q}} [1-\exp(-Aq^2)]\sigma(\mathbf{q})\, dq_\perp^2 dq_z d\varphi dK = d\sigma_i + d\sigma_c, \tag{27}$$

where

$$\sigma(\mathbf{q}) = [1+(1-x)^2]F_1 - \tfrac{2}{3}(1-x)F_2.$$

For the polarization we get

$$(d\sigma_\perp - d\sigma_{||}) = P d\sigma_{\text{cry}} = (\sigma_0/K)2(1-x)(2\pi/a)^3 N_1N_2N_3 \sum_{\mathbf{g}} |S|^2 \int_{\mathbf{q}} \delta(\mathbf{q}-\mathbf{g}) \exp(-Aq^2) \cos 2\varphi' F_3 dq_z dq_\perp^2 d\varphi dK. \tag{28}$$

We see (27) splitting into two terms; that is, $d\sigma_{\text{cry}} = d\sigma_i + d\sigma_c$, the first of which represents the coherent or interference part of the cross section, and the second one represents the continuous or amorphous part, dependent only on the temperature through A.

The value for $d\sigma_c$, computed in Überall's paper,[5] gives

$$d\sigma_c = (\sigma_0/K)\{[1+(1-x)^2]\psi_{1c} - \tfrac{2}{3}(1-x)\psi_{2c}\}dK; \tag{29}$$

in the complete-screening approximation ($\delta\beta \ll 1$) the functions are

$$\psi_{1c} = 2[2\ln\beta + (1-D)e^D E_i(-D) + 2],$$

$$\psi_{2c} = 2[2\ln\beta + (1+D)e^D E_i(-D) + \tfrac{5}{3}],$$

$$\beta = 111 z^{-1/3}, \quad D = A\beta^{-2}, \quad E_i(-D) = -\int_D^\infty \frac{e^{-t}}{t}\, dt. \tag{30}$$

These functions, upon fixing the temperature, crystal (that is, A), and atomic number Z (that is, β), are constant. In (28) the continuous part disappears because

$$\sigma_c \int_0^{2\pi} \cos 2\varphi' d\varphi = 0.$$

Now we consider the polarization with respect to the plane $(\mathbf{p}_1, \mathbf{b}_1)$ (which we call the incidence plane) instead of to the plane $(\mathbf{q}, \mathbf{p}_1)$ (recoil plane). We call φ' the angle between the two planes, and so we have $\varphi' = \varphi - \alpha$ [see Fig. 9(b)], where α is the angle between

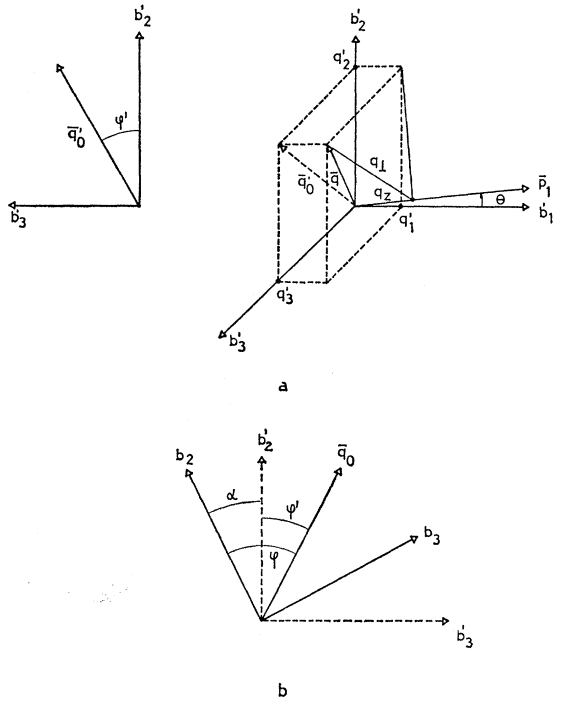

FIG. 9. (a) The case in which the incidence plane is coincident with the crystal plane, or $(b_1', b_2') \equiv (\mathbf{p}_1, b_1')$; the primes denote the special case we have chosen. (b) General case for which the plane $(\mathbf{p}_1, \mathbf{b}_1)$ makes an angle α with the plane $(\mathbf{b}_2, \mathbf{b}_1)$. In both figures $q_0 = q_0' = (q_2^2 + q_3^2)^{1/2} \approx q_\perp$. The vertical hatched line is the intersection with the plane $(\mathbf{p}_1, \mathbf{b}_1)$.

the crystal plane ($\mathbf{b}_1$, $\mathbf{b}_2$) and the incidence plane, and φ is the angle between the recoil plane and the crystal plane ($\mathbf{b}_1$, $\mathbf{b}_2$). In doing so we take the vector $\mathbf{b}_{1\perp}$ (Fig. 8) in this crystal plane. In order to understand the reason for the factor $\cos 2\varphi'$ in (28), we remember that if P_0, P are the polarizations of a beam of particles with respect to two planes π_0, π, making an angle φ' in-between, then the following relation holds: $P=P_0 \cos 2\varphi'$.

As far as the interference part of the cross section is concerned, the first integration in (27) and that in (28) consists in evaluating the integral

$$\int_{\mathbf{q}} \delta(q_1-g_1)\delta(q_2-g_2)\delta(q_3-g_3)F_1 \exp(-Aq^2)\,dq_z dq_\perp{}^2 d\varphi \tag{31}$$

and two others for F_2, $F_3 \cos 2\varphi'$ functions. Here q_1, q_2, q_3, g_1, g_2, g_3 are the components of the recoil momentum and of the reciprocal lattice vectors along the axis b_1, b_2, b_3 of the lattice. In the first Überall papers[5,6] an approximation was used in which the lattice planes perpendicular to the b_1 axis were considered as continuous planes. This corresponds to taking as the Dirac function $\delta(\mathbf{q}-\mathbf{g})=\delta(q_1-g_1)$ and integrating continuously over q_2, q_3. In the experimental research of the Frascati group, it was shown that this approximation does not work for 1-GeV bremsstrahlung and that it is necessary to take into account the actual structure of the lattice. In this way higher polarization would have been available at the top of very large and sharp peaks in the bremsstrahlung spectrum.

After this the intensity and polarization were computed and measured[14,16,17,19–21] at Frascati. A contemporary calculation of the polarization has been computed by Überall.[18] In the following we show the calculation of the intensity and polarization by using the complete Dirac function

$$\delta(\mathbf{q}-\mathbf{g})=\delta(q_1-g_1)\delta(q_2-g_2)\delta(q_3-g_3).$$

In order to perform the integrations (31), with the help of the Dirac functions, we have to express q_1, q_2, q_3 (in the arguments of the Dirac functions) through the variables of integration q_z, $q_\perp{}^2$, φ.

Also, we have to introduce the fundamental "incidence angle" $\theta=\sphericalangle(\mathbf{p}_1, \mathbf{b}_1)$. Since $\theta \approx \delta a_{\text{cry}}$ this is a small angle, and so we may put $\sin\theta\approx\theta$, $\cos\theta\approx 1$.

For this, we proceed through a two-step process. First, suppose the crystal plane ($\mathbf{b}_2$, $\mathbf{b}_1$) is coincident with the incidence plane ($\mathbf{p}_1$, $\mathbf{b}_1$). From an inspection of Fig. 9(a) we obtain

$$\begin{aligned} q_z &= q_1'+\theta q_2', \qquad q_\perp{}^2 = q_2'^2+q_3'^2, \\ \cos 2\varphi' &= (q_2'^2-q_3'^2)/(q_2'^2+q_3'^2), \\ \cos\varphi' &= q_2'/(q_2'^2+q_3'^2)^{1/2} \approx q_2'/q_\perp, \end{aligned} \tag{32}$$

where the primes indicate the special condition chosen.

As a second step, rotate the reference axes (b_1', b_2', b_3') of Fig. 9(a) by an angle α around the axis b_1'. We obtain the new axis $b_1'\equiv b_1$, b_2, b_3 of Fig. 9(b). The old coordinates as a function of the new axis are

$$\begin{aligned} q_1' &= q_1, \qquad q_2' = q_2\cos\alpha+q_3\sin\alpha, \\ q_3' &= q_3\cos\alpha-q_2\sin\alpha. \end{aligned}$$

Thus, the expressions (32) become

$$\begin{aligned} q_z &= q_1+\theta(q_2\cos\alpha+q_3\sin\alpha), \qquad q_\perp{}^2 \approx q_2^2+q_3^2, \\ \cos 2\varphi' &= \cos 2(\varphi-\alpha) = [(q_2^2-q_3^2)/(q_2^2+q_3^2)]\cos 2\alpha + 2\sin 2\alpha[q_2q_3/(q_2^2+q_3^2)], \\ \cos\varphi' &= (q_2\cos\alpha+q_3\sin\alpha)/(q_2^2+q_3^2)^{1/2}. \end{aligned} \tag{33}$$

By using (33) and the properties of the Dirac functions we obtain

$$\begin{aligned} \delta(q_1-g_1)\delta(q_2-g_2)\delta(q_3-g_3) &= 8\sin 2\varphi'\delta\{q_z-[\theta(g_2\cos\alpha+g_3\sin\alpha)+g_1]\} \\ &\times\delta(\cos 2\varphi'-\{[(g_2^2-g_3^2)/(g_2^2+g_3^2)]\cos 2\alpha+[g_2g_3/(g_2^2+g_3^2)]2\sin 2\alpha\})\delta[q_\perp{}^2-(g_2^2+g_3^2)]. \end{aligned} \tag{34}$$

To complete the integration, it is sufficient to make (multiplied by 2) the following substitutions in the functions:

$$\begin{aligned} q_z &\to [\theta(g_2\cos\alpha+g_3\sin\alpha)+g_1], \qquad q_\perp{}^2 \to (g_2^2+g_3^2), \\ \cos 2\varphi' &\to [(g_2^2-g_3^2)\cos 2\alpha+g_2g_3 2\sin 2\alpha]/(g_2^2+g_3^2). \end{aligned}$$

We summarize the results for the bremsstrahlung cross section and for polarization:

$$\begin{aligned} d\sigma_{\text{cry}}^{(b)}/dK &= (d\sigma_i/dK)+(d\sigma_c/dK) \\ &= (\sigma_0/K)\{[1+(1-x)^2](\psi_1+\psi_{1c})-\tfrac{2}{3}(1-x)(\psi_2+\psi_{2c})\}, \end{aligned} \tag{35a}$$

$$\begin{aligned} P(d\sigma_{\text{cry}}^{(b)}/dK) &= [(d\sigma_\perp/dK)-(d\sigma_{||}/dK)]_{\text{cry}} \\ &= (\sigma_0/K)2(1-x)\psi_3. \end{aligned} \tag{35b}$$

Putting $B=4(N_0/N)[(2\pi)^2/a^3]$, the functions ψ_i are

$$\psi_1=B\sum_{\mathbf{g}} |S|^2 \exp(-Ag^2)F(q^2)\delta(g_2^2+g_3^2)/[\theta(g_2\cos\alpha+g_3\sin\alpha)+g_1]^2,$$

$$\psi_2=6B\sum_{\mathbf{g}} |S|^2 \exp(-Ag^2)F(q^2)\delta^2(g_2^2+g_3^2)[\theta(g_2\cos\alpha+g_1\sin\alpha)+g_1-\delta]/[\theta(g_2\cos\alpha+g_3\sin\alpha)+g_1]^4,$$

$$\psi_3=B\sum_{\mathbf{g}} |S|^2 \exp(-Ag^2)F(g^2)\delta^3[(g_2^2-g_3^2)\cos 2\alpha+\sin 2\alpha g_2g_3]/[\theta(g_2\cos\alpha+g_3\sin\alpha)+g_1]^2. \tag{36}$$

We remember that $g_i=h_i(2\pi/d_i)$ (h_i is an integer number) and the sums in (36) are extended over the triplet $\mathbf{g}(g_1, g_2, g_3)$, under the condition $q_z\geq\delta$; that is,

$$g_1+(g_2\cos\alpha+g_3\sin\alpha)\theta\geq\delta. \tag{37}$$

The functions (36) may be simplified by using the approximation of considering as effective only the first plane of the reciprocal lattice and by choosing the orientation of the crystal represented in Fig. 9(a).

In this way we have $g_1=0$ and $\alpha=0$. The $g_1=0$ approximation is justified by the q_z^{-2} or q_z^{-4} dependence of (36). Thus we get, after putting $\tau=\theta/\delta$,

$$\chi_1^0(\tau)=B\sum_{g_2,g_3} |S|^2 \exp(-Ag^2)F(q^2)(g^2/g_2^2\tau^2)=\psi_1^0\delta,$$

$$\chi_2^0(\tau)=6B\sum_{g_2,g_3} |S|^2 \exp(-Ag^2)F(q^2)(g^2/g_2^4\tau^4)(\tau g_2-1)=\psi_2^0\delta,$$

$$\chi_3^0(\tau)=B\sum_{g_2,g_3} |S|^2 \exp(-Ag^2)F(q^2)(g_2^2-g_3^2/g_2^4\tau^4)=\psi_3^0\delta, \tag{38}$$

where the index (0) indicates that the χ^0 functions are related only to the plane $g_1=0$. For bremsstrahlung in the range of 1 GeV or more, the contributions of the planes $g_1=h_1(2\pi/a_1)$ for $h_1\neq 0$ are completely negligible. The condition (37) now becomes $g_2\gg 1/\tau$.

The polarization P of the coherent bremsstrahlung with respect to the incidence plane ($\mathbf{p}_1$, $\mathbf{b}_1$) may be derived from (35b). We get

$$P=\frac{2(1-x)\psi_3}{[1+(1-x)^2](\psi_1+\psi_{1c})-\frac{2}{3}(1-x)(\psi_2+\psi_{2c})}. \tag{38'}$$

Let us suppose again that $\psi_{1c}\approx\psi_{2c}\approx 0$, corresponding to a high Debye temperature and a low crystal temperature, and that only the point of the reciprocal lattice $\mathbf{g}'=\mathbf{g}_1'+\mathbf{g}_2'+\mathbf{g}_3'$ be effective. Also let us consider the polarization value just at the top of the corresponding peak, by which we have $q_z=\delta$ or

$$g_1+(g_2\cos\alpha+g_3\sin\alpha)\theta=\delta.$$

Under these limitations we have

$$\tilde{P}_{g'}=\frac{2(1-x)}{1+(1-x)^2}\left(\frac{g_2'^2-g_3'^2}{g_2'^2+g_3'^2}\cos 2\varphi+\frac{2g_2'g_3'}{g_2'^2+g_3'^2}\sin 2\alpha\right)=\frac{2(1-x)}{1+(1-x)^2}\cos 2(\varphi_{g'}-\alpha). \tag{39}$$

For $\varphi'=\varphi-\alpha=0$ this expression reduces to (26).

B. Electron Pair Production in Crystals

Calculation of the coherent electron pair cross section may follow, step by step, the same procedure as for the bremsstrahlung case.

Let us suppose an incident polarized photon beam of momentum $\mathbf{K}$ is hitting an amorphous target. Let us call $\boldsymbol{\varepsilon}$ the polarization vector normal to the photon's direction and consider only those electron pair production processes in which the recoil momentum has the same well-defined value $\mathbf{q}$. We can express the May[29] cross section, as in the bremsstrahlung case, as a function of the variables $q_\perp^2$, q_z, φ, β, where now $q_\perp$, q_z are the components of $\mathbf{q}$ perpendicular and parallel to the $\mathbf{K}$ direction, φ is the angle between the ($\mathbf{K}$, $\mathbf{q}$) plane and a fixed plane, and β is the angle between the polarization plane ($\boldsymbol{\varepsilon}$, $\mathbf{K}$) and the recoil plane ($\mathbf{q}$, $\mathbf{K}$). If we put, in this expression, $\beta=0$ or $\pi/2$, we obtain for the corresponding cross sections $\sigma_{||}$ and $\sigma_\perp$ two expressions similar to those in the bremsstrahlung case. The results concerning the sum and difference are

$$d^4\sigma_{||}+d^4\sigma_\perp=\sigma_0\{[y^2+(1-y)^2]F_1+2y(1-y)F_2\}\times dq_z dq_\perp^2 d\varphi dy,$$

$$d^4\sigma_{||}-d^4\sigma_\perp=-\sigma_0 2y(1-y)F_3 dq_z dq_\perp^2 d\varphi dy. \tag{40}$$

Here, $y=E_\pm/K$ is the ratio between the energies of one electron of the pair and of the photon producing the pair. The functions F_1, F_2, F_3 are exactly the same functions we have seen in the bremsstrahlung case, (24). But now we have $\delta=[2Ky(1-y)]^{-1}$. Since the second (20) is always negative, it follows that the cross section for emission of electron pairs is higher when $\boldsymbol{\varepsilon}\perp\mathbf{q}_\perp$ than in the case when $\boldsymbol{\varepsilon}\,||\,\mathbf{q}_\perp$. As in the bremsstrahlung case, we now consider the electron pair

production in a single crystal. As before we consider first that only a point of the lattice be effective and that there is no contribution from the incoherent part of the cross section (no thermal vibrations at all). Then, we may write immediately the asymmetry ratio R_q for the electron pair production in a crystal under the previous restrictive conditions; that is,

$$R_{q_i}=[(d^4\sigma_{||}-d^4\sigma_\perp)/(d^4\sigma_{||}+d^4\sigma_\perp)]_{(q_i,K)} = \frac{2y(1-y)F_3}{[y^2+(1-y)^2]F_1+2y(1-y)F_2}. \quad (41)$$

This asymmetry ratio is computed with respect to the plane $(\mathbf{K}, \mathbf{q})$. Also in this case, if we consider this ratio in correspondence of peak of the EPP cross section, in which $q_z=\delta$, and thus $F_2=0$, $F_1=F_3$, we obtain

$$R_{q_i,q_z=\delta}=2y(1-y)/[y^2+(1-y)^2]=1 \quad \text{for} \quad y=\tfrac{1}{2}.$$

The conditions in which these asymmetry ratios are valid are much more unrealistic than in the bremsstrahlung case.

It is interesting to know, in any case, that the existence of an asymmetry ratio in the high-energy EPP allows us in principle to use a crystal as analyzer for measurements of the polarization of high-energy photons. We now derive the general expression for the cross section of the EPP in a single thin cubic crystal. Let us have a high-energy photon beam of momentum $\mathbf{K}$ linearly polarized in the direction $\boldsymbol{\varepsilon}$ and striking the crystal at a small angle θ (≤ 0, 1 rad) with a reciprocal lattice axis $\mathbf{b}_1$. Let us call φ the angle between the plane $(\mathbf{q}, \mathbf{K})$ and the plane $(\mathbf{b}_2, \mathbf{b}_1)$ [see Figs. 9(a), 9(b)]. If we proceed exactly in the same way as in the bremsstrahlung case, we obtain

$$d\sigma_{||}-d\sigma_\perp=\sigma_0 2y(1-y)\psi_3(\theta,\delta,\alpha)dy, \quad (42a)$$

$$d\sigma_{||}+d\sigma_\perp=\{[y^2-(1-y)^2][\psi_1(\theta,\delta,\alpha)+\psi_1{}^c(\delta)] + \tfrac{2}{3}y(1-y)[\psi_2(\theta,\delta,\alpha)+\psi_2{}^c(\delta)]\}\sigma_0 dy, \quad (42b)$$

where the functions ψ_1, ψ_2, ψ_3 and $\psi_1{}^c$, $\psi_2{}^c$ are given in (36) and (30), and where $\delta=[2Ky(1-y)]^{-1}$.

C. Some Numerical Results

In order to obtain numerical results it is necessary to choose an actual crystal. Only crystals with a diamond lattice were used in the experiments performed until now, i.e., germanium, silicon, and diamond. We show examples related to diamond crystals extensively used in the experiments on the high-energy coherent bremsstrahlung by 1- and 6-GeV electrosynchrotrons. This choice was made because the diamond lattice has a high Debye temperature $\theta=1860$°K, and thus a low value of the quadratic thermal displacement $A=126\lambda_c{}^2$, and a relatively small lattice constant $a=922\lambda_c=3.56$ Å. We need to take an explicit expression for the form factor of the carbon atom. For a first approximation it is sufficient to take the Schiff exponentially screened

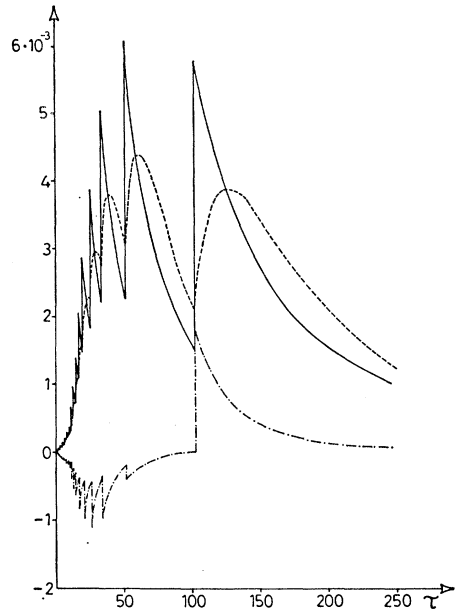

FIG. 10. Numerical values of the functions $\chi_1{}^0$(——), $\chi_2{}^0$(– – –), $\chi_3{}^0$=(–·–·–), versus $\tau=\theta/\delta$. The incident electron momentum $\mathbf{p}_1$ lies in the [110][1$\bar{1}$0] plane; that is, $\alpha=\pi/2$ (exponential screening).

model of the form factor; that is, $F(g^2)=(\beta^{-2}+g^2)^{-2}$, where $\beta=111\times z^{-1/3}$. This model was used in all the first calculations of the Überall and Frascati staffs. Some more sophisticated models have been used in more recent work.[23,24,26] The following results are presented.

Figure 10: The functions $\chi_1{}^0$, $\chi_2{}^0$, $\chi_3{}^0$ given by (38) are reported versus $\tau=\theta/\delta$. The incident particle's momentum $\mathbf{p}_1$ lies in the plane [110][1$\bar{1}$0]. Only the plane through ($h_1=0$) is taken into account. Exponential screening is used. This is essentially the situation of Fig. (3).

Figure 11: The same functions are obtained as in Fig. 10, but the momentum $\mathbf{p}_1$ now lies in the plane [110][001]. These curves are obtained by substituting $g_3\rightarrow g_2$ in (38). For $\tau=146$ (Fig. 11) there is a sharp discontinuity due to the row of reciprocal points nearer to the origin. In a situation in which this discontinuity appears, the conditions $\theta_1=146[x/2E_0(1-x)]$ and $\theta_1=146(1/2K)[1/y(1-y)]$ must be fulfilled: For fixed x and y values the angle θ_1 decreases when the primary energy increases.

Figure 12: A bremsstrahlung spectrum and polarization is shown at $E_0=5.5$ GeV, $\theta=8$, 18 mrad, calculated with exponential screening (solid line) and with a Hartree-type model (dotted line) of the form factor.[23] The orientation is the same as in Fig. 11. As was shown in the previous sections, higher polarization values could be obtained by choosing a crystal orientation by which only a point of the crystal lattice is effective. A Desy group of physicists[23] showed that this goal is reached by choosing a very large angle θ and by

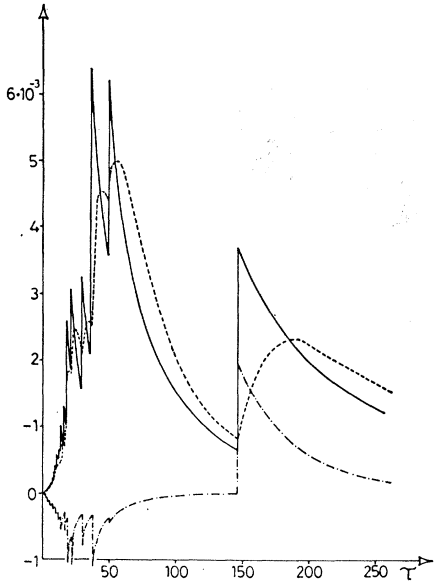

FIG. 11. The same as Fig. 10, but now the $\mathbf{p}_1$ vector lies in the plane [110][001]; that is, $\alpha=0$.

rotating the crystal by an angle α around the $\mathbf{p}_1$ direction.

Figure 13: The functions $\delta\psi_1$, $\delta\psi_2$, $\delta\psi_3$ are shown as given by (36), obtained for $\alpha=13°\ 26'$. For $\tau=226$ we have the main peak of $\delta\psi_1$, $\delta\psi_2$ functions which give, in the 1-GeV bremsstrahlung spectrum, a peak at $x=0.150$ with 75% maximum polarization, mainly due to the point $h_1=h_2=0$, $h_3=2$; that is, the second point along the $[1\bar{1}0]$ axis (see Fig. 4). Bremsstrahlung spectra and polarizations of this kind are shown in the next section, together the experimental results.

Figure 14: In Fig. 14 the ratio

$$R_c=(d\sigma_{||}-d\sigma_{\perp})/(d\sigma_{||}+d\sigma_{\perp})$$

[given by (42a) and (42b)] is shown as a function of the angle θ, together the electron pair production cross section values for $K=3$ GeV, $y=\frac{1}{2}$, and $\alpha=0$.

IV. MEASUREMENTS OF COHERENT ELECTRON PAIR PRODUCTION AND HIGH-ENERGY BREMSSTRAHLUNG CROSS SECTIONS

The next section deals with the experimental problem involved in the measurements and exploitation of the coherent HEB and EPP. Let us consider first the measurements on the unpolarized bremsstrahlung and EPP cross sections. The main task is the measurement of the energy dependence of the bremsstrahlung and EPP cross sections for fixed angle of incidence θ and the θ dependence of the cross sections for fixed photon energy K.

Mainly in the bremsstrahlung case high-energy resolution is needed, of the order of few percent in $\Delta K/K$, and also an accurate measurement of the angle θ. The first may be accomplished in two ways:

(a) By measuring directly the photon energy by converting it in electron pairs inside a good magnetic spectrometer, or

(b) by measuring the energy E of the recoil electron.

In fact $K=E_0-E-E_q$, but the very small energy of the recoil nucleus $E_q=q^2/2M$ may be neglected and the primary energy E_0 is the usually well-known energy of the electron accelerator. For circular accelerators with an internal electron beam and a large duty cycle, the solution (a) is convenient. In fact the large duty cycle allows measurements with good statistical accuracy, low accidental counting rate in electron–positron coincidences, and high-energy resolution. On the other hand, if there is only an internal electron beam, it is difficult to pick up the recoil electrons from a crystal placed inside a straight section. On the contrary, when external electron beams and short duty cycles are available, as in the linear-accelerator case, the method (b) could possibly be used. Because of the short duty cycle both methods of measurement require some reduction of the bremsstrahlung intensity, i.e., of the crystal thickness or of the electron beam intensity, or of the converter thickness and detection efficiency.

The Frascati measurements and those of other laboratories have been carried out until now by the electron pair conversion method only. The primary

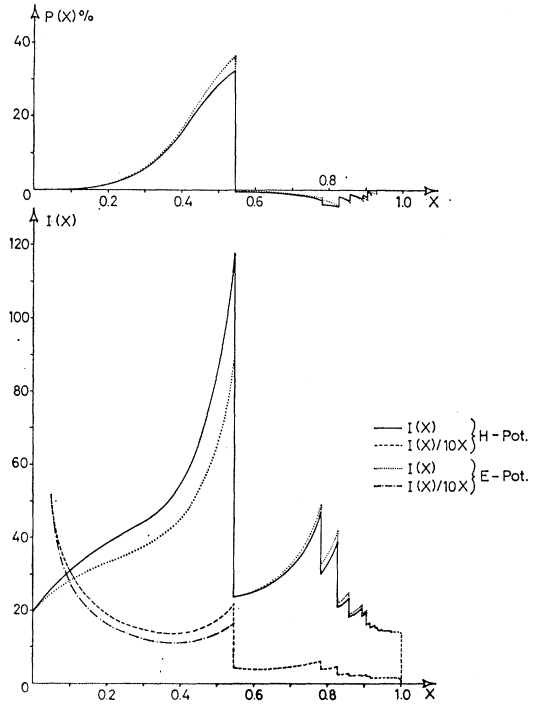

FIG. 12. Bremsstrahlung spectrum and ploarization at $E_0=5.5$ GeV, $\theta=8.176$ mrad, computed with an exponential form factor (E-Pot.) and with a Hartree-type model (H-Pot.) of the form factor (see Ref. 23). The vector $\mathbf{p}_1$ lies in the plane [110][001]; that is, $\alpha=0$. Only the plane through $h_1=0$ is taken into account. The values $\psi_1^c=14.60$, $\psi_2^c=13.90$ are used. (Courtesy of G. Bologna.)

electron beam divergence and Coulomb scattering in the crystal target before radiating causes a spread in the values involved in each bremsstrahlung process. Let us suppose we have a pointlike radiator and an infinitely narrow collimation angle α_c or, experimentally, $\alpha_c \ll \alpha_b = mc^2/E$, where α_b is the "natural" angle of the bremsstrahlung. Then the parent electrons of the photons in the collimated bremsstrahlung make a maximum angle of $\alpha_b \cong 1/E$, with the photon beam itself. Thus, the relative spread in the angle θ is $\alpha_b/\theta \propto 2(1-x)/x$, no matter how large the primary electron divergence or the Coulomb scattering in the crystal (pointlike radiator). Moreover, the ratio α_b/θ is independent of the primary energy E of the electrons. This is the main reason by which large and polarized peaks of photons are expected up to very high energy of the primary electrons.[22] In Fig. 15 the experimental arrangement used by the Frascati staff[10,11,19,20] at the 1-GeV electron synchrotron is shown. A crystal CR is placed inside a straight section of the Frascati synchrotron. The collimated Bremsstrahlung beam enters a vacuum pipe and the vacuum chamber of a pair spectrometer and dies in a Wilson quantameter. At the entrance of the vacuum chamber a converter is located. The symmetrical electron pairs produced in the converter are detected by plastic scintillators A_1, A_2, A_3 placed along two electron trajectories of the same energy and opposite charge, at 1 m from the end of the magnet. This energy is fixed by the magnetic-field value inside the pair spectrometer and so the photon energy $K = E_+ + E_-$ is known. C_1, C_2, C_3 are three lead collimators with different tasks. The collimator C_2 which actually defines the γ-beam dimensions has a variable aperture of 0.2–1 mrad with respect to the radiator position.

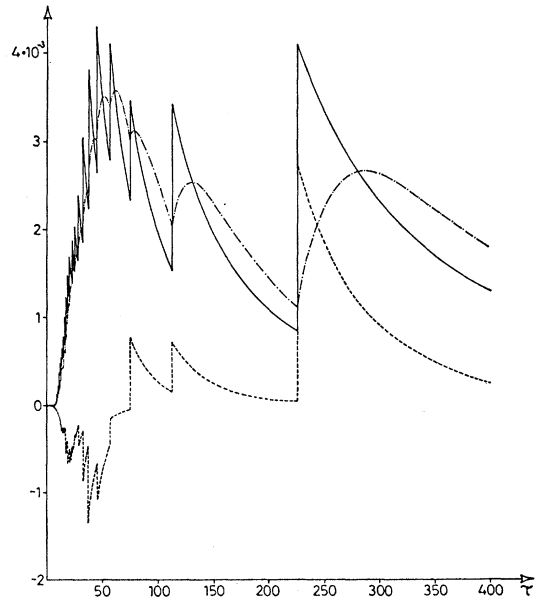

FIG. 13. Numerical values of the functions $\delta\psi_1^0$(——), $\delta\psi_2^0$(-·-) $\delta\psi_3^0$(- - -), versus $\tau = \theta/\delta$, for $\alpha = 13°\ 26'$; exponential form factor. Only the plane through $h_1 = 0$ is taken into account. (Courtesy of G. Bologna.)

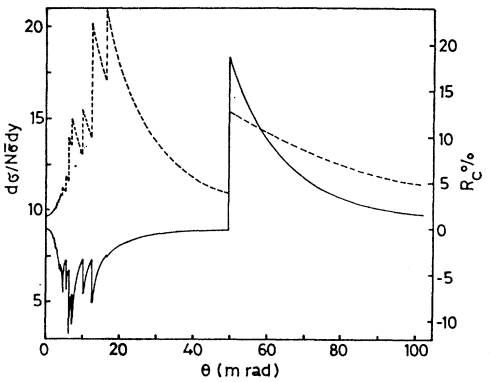

FIG. 14. Electron pair production from $K = 3$ GeV linearly polarized photons in a diamond crystal.[21] The solid line represents the asymmetry ratio R_c given in the text (read at the right scale). The photon momentum **K** lies in the plan [110][001]. The dashed curve is the EPP cross section for unpolarized photons (read at the left scale) for symmetrical pairs. The abscissa gives the θ values, angle [110], **K**. (Ref. 22.)

C_1 has an angle of 2.5 mrad in order to decrease the number of photons hitting the lead of C_2. In fact these photons generate electromagnetic showers in C_2, and this collimator becomes a source of particles and photons of degraded energy so that the broom magnet B is unable to sweep out. The collimator C_3, with an aperture angle of $\sim$3 mrad, stops most of these particles. The vacuum chamber is closed in the back by a Mylar window of 5×10^{-4} radiation length. The electron pairs generated in this unwanted target and deflected by the fringing field of the magnet are stopped by two lead vertical plates P. Of course this experimental arrangement is suitable for both bremsstrahlung and EPP measurements. First we report the results obtained by the Frascati staff concerning the coherent EPP measurements. A silicon crystal in the form of a plate 18 mm diam and 0.08 mm thick was placed at the entrance of the spectrometer vacuum chamber, as an electron–positron converter.

The radiator inside the synchrotron-producing bremsstrahlung is a usual tantalum plate of 0.13 radiation length. A goniometric device allows the crystal to be rotated around a vertical and an horizontal axis. The first experiment consisted in measuring the number $N(\theta)$ of symmetrical pairs per fixed number of monitor units as a function of the angle θ between the crystal axis [100] and the photon direction. In Figs. 16(a), (b) the results[10] relative to rotation of the silicon crystal about the horizontal and vertical axis are shown. The points of the figures are given by

$$\rho(\theta) = [N(\theta, K) - N(0, K)]/N(0, K),$$

where

$$N(\theta) = N_P(\theta) - N_d(\theta) + (N_{fp} - N_{fd}).$$

$N_P(\theta) = A_1 + A_2 + A_3$ and $N_d(\theta) = A_1 + (A_2 + A_3)_d$ are the numbers of prompt and delayed coincidences due to the single crystal and N_{fp}, N_{fd} the same quantities due to the background without crystal. At the time of these experiments the problem of the fine structure

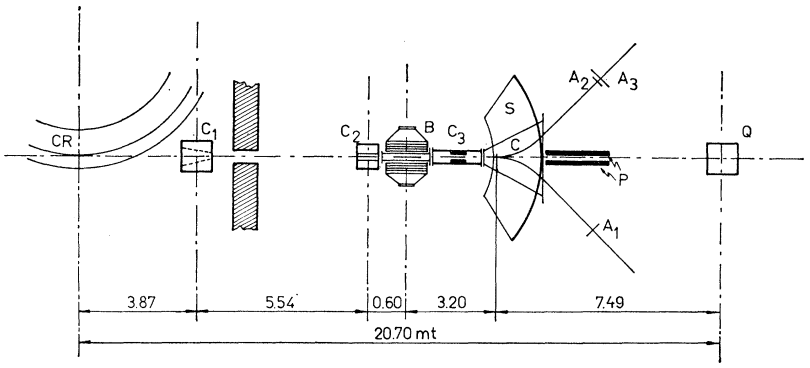

FIG. 15. Experimental setup used by the Frascati group for measuring the coherent HEB and EPP (see text).

was not raised. Therefore, the continuous curves in the figures are derived from the Überall result concerning continuous lattice planes. The function representing the curves is

$$\eta(\theta)=\frac{[\phi_n(\theta)+\phi_e](1+\frac{1}{2}\theta^2)-\phi_n(0)+\phi_e}{\phi_n(0)+\phi_e},$$

where $\phi_n(\theta)$ and ϕ_e are quantities proportional to the EPP cross section in the field of the nucleus and electron, respectively. $\phi_n(\theta)$ is defined by

$$\phi_n(\theta)=[y^2+(1-y)^2][\psi_1{}^c+\psi_1{}^0(\theta/\delta)]+\tfrac{2}{3}y(1-y)[\psi_2{}^c+\psi_2{}^0(\theta/\delta)],$$

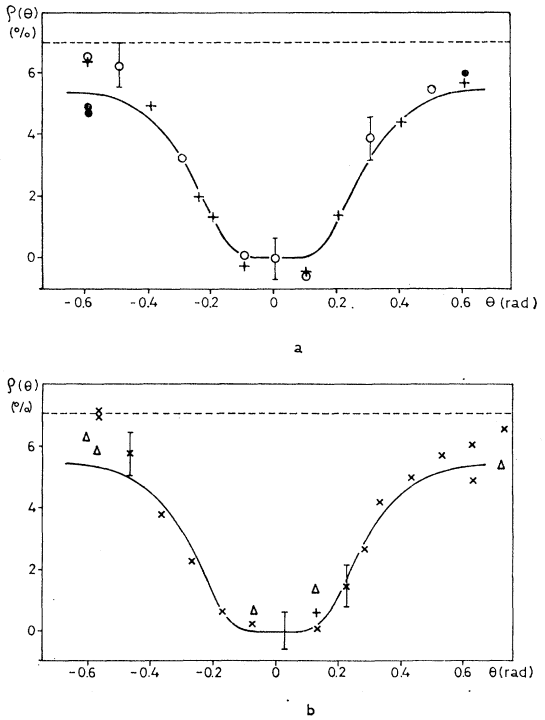

FIG. 16. Relative variation of the electron pair production cross section in a silicon single crystal versus θ (angle between γ-ray direction and the crystal axis [100]). The solid line represents the function $\eta(\theta)$ given in the text. The central energy of the incident photon is $K=910$ MeV. The experimental points represent ρ (θ) given in the text. Different runs of measurements are related to different shape of the dots. Parts (a) and (b) refer to rotations of the crystal about the horizontal and vertical axis, respectively (see the text or Ref. 10). The α value is unknown.

where $y=E_\pm/K=0.5$, $E_\pm=455$ MeV is the central energy of the electrons, and $K=910$ MeV the photon energy; $\psi_1{}^c$, $\psi_2{}^c$, $\psi_1{}^0$, $\psi_2{}^0$ are *not* the functions computed before in Sec. II, but those calculated by Überall.[5] The contribution of the atomic electrons is taken from the Wheeler–Lamb formula

$$\phi_e=(1.33/Z)\phi_{\rm BH},$$

where $\phi_{\rm BH}$ is proportional to the Bethe–Heitler EPP cross section. The factor $(1+\frac{1}{2}\theta^2)$ takes into account the variation of the effective thickness due to the rotation of the angle $\theta(<0.07$ rad). In fact the minimum recoil momentum is much larger than in the bremsstrahlung case. We have (see Table I) $\delta=10^{-3}$ and $2\pi/a=4.5\times10^{-3}$ for a silicon crystal. Thus the ratio $2\pi/a\delta\simeq4.5$, and if we consider $\theta=0.02$ rad, there will be about 10^2 reciprocal lattice points in the recoil momentum region, and so discontinuities due to the displacement of single points are undetectable by this experimental resolution. This experiment showed for the first time the existence of the central minimum expected according to the Überall calculations.

Other sets of measurements have been carried out by the Frascati staff at fixed θ for different energies of the photons, obtained by changing the magnetic field in the

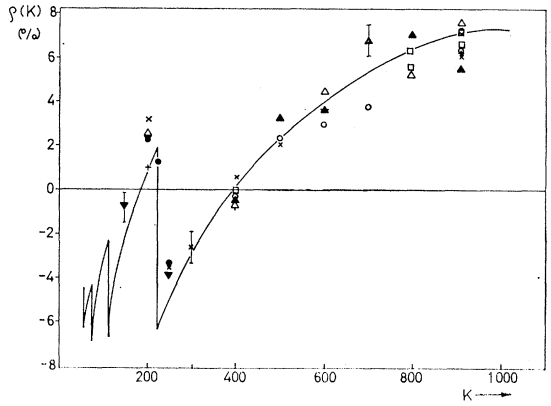

FIG. 17. The ratio $\rho=N[(\theta_0, K)-N(0, K)]/N(0, K)$, with $\theta_0=60$ mrad, is given versus the photon energy K_1, for a silicon crystal. Solid line gives the theoretical curve computed by using the Überall functions.[6] The inversion in the sign of ρ is due to the second lattice plane. The different shape of the dots refer to different experimental runs (Frascati results).

pair spectrometer. More exactly, the ratio $\rho(\theta, K)$ has been measured for $\theta=0$ and $\theta=60$ mrad at different K values. The results are reported in Fig. (17). There is agreement with the theoretical curve again computed with the Überall functions.[5] The inversion in the sign of $\rho(\theta, K)$ and its sharp discontinuity are very interesting. Both effects are due to the existence of the second lattice plane through $h_1=1$. As K decreases, $\delta \propto (1/K)$ increases and the recoil momentum region goes over the second lattice plane. In this situation, for $\theta=0$ we have just a central maximum for the cross section, i.e., $N(\theta=0, K)>N(\theta=60$ mrad, $K)$ for K small enough or for $\delta\sim 2\pi/a$.

When δ becomes equal to the distance between the planes through $h=0$ and $h=1$, the second lattice planes leave the recoil momentum region, and for $\theta=0$ we get a new central minimum. This happens when $\delta=2\pi/a$, or $K=2(a/2\pi)mc^2=226$ MeV for the silicon along the [100] axis. We reported these results here because they are the only clear experimental evidence of a second lattice plane interference effect.

Now we summarize and comment on some of the experimental results obtained on coherent HEB. We begin with the results of the Frascati staff[11,19] which showed, as was stated before, the influence on EPP and HEB of the actual structure of the lattice planes. One of the first important results[19] concerning the interference bremsstrahlung spectrum with the typical peaked structure is shown in Fig. 18. In order to do this experiment, a diamond crystal having a shape of a $(10\times5\times2)$ mm^3 parallelepiped was placed in the straight section of the Frascati synchrotron as a radiator. It was mounted in a remote-controlled goniometer in order to make possible and to measure rotations about horizontal and vertical axes, both perpendicular to the electron beam direction. The crystal axis $[1\bar{1}0]$ is placed along the former direction and the axis [001] along the latter within $\pm2°$. The axis [110] is perpendicular to the widest faces of the diamond and makes an angle θ with the electron beam striking the crystal. The goniometric device was much improved with respect to the preceding one used in the first interference bremsstrahlung measurements (see Ref. 11). It now has a sensitivity of 0.1 mrad and the angles are measured with a relative systematic error of $\pm0.1\%$. The γ-ray beam strikes an aluminum converter 1.1×10^{-3} radiation length in thickness. According the to crystal orientation explained before, when the crystal is rotated about a vertical direction, the intersection of the momentum space region with the lattice plane is a line parallel to the [001] axis as in Fig. 3.

The spectrum showed in Fig. 18(a) has been measured, with the above condition, at an angle $\theta=\theta_1=4.6\pm0.1$ mrad, and the others in Fig. 18(b) at angles $\theta=\theta_2=11.3\pm0.1$ mrad and $\theta=\theta_3=22.9\pm0.1$ mrad. The experimental data represents the quantity

$$J_{\text{exptl}}(K,\theta)=[N(K,\theta)\sigma_P(K_0)/N(K_0,\theta)\sigma_P(K)][f(K)],$$

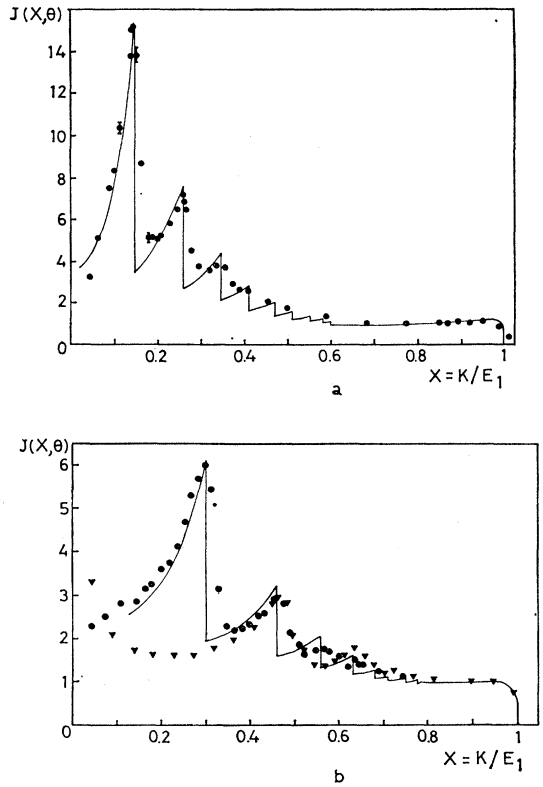

FIG. 18(a) Bremsstrahlung intensity for $E_0=1$ GeV in a diamond crystal. The incident momentum $\mathbf{P}_1$ lies in the plane $[110][1\bar{1}0]$ and makes the angle $\theta=\theta_1=4.6\pm0.1$ mrad with the axis $[1\bar{1}0]$, i.e., $\alpha=\pi/2$. Solid line is the theoretical curve without any correction. The experimental points are given by the expression J_{exptl}. given in the text. (b) The same situation as in (a), but $\theta=\theta_2=11.3\pm0.1$ mrad for the dots and solid line, and $\theta=\theta_3=22.9\pm0.1$ for the triangles (Frascati results, Ref. 19).

where $K_0=900$ MeV is the photon energy at which normalization is performed. By $\sigma_P(K)$ we mean the symmetrical pair production cross section in aluminum, viz., the sum of the contribution due to nuclei and electrons.

The correction factor $f(K)$ takes into account the scintillator vertical counting losses. The solid curves represent the theoretical quantity

$$J_{\text{th}}(x,\theta)=I(x,\theta)/I(x_0,\theta),$$

where $x_0=K_0/E_1$, $x=K/E_1$ with $E_1=1$ GeV the electron energy, and $I(x,\theta)=K(d\sigma_{\text{cry}}/dK)$, with $d\sigma_{\text{cry}}/dK$ given by the first of (35) and from the first two equations of (38). The agreement is quite good also, if the following remarks are kept in mind:

(a) The theoretical curves are not corrected for the energy spread of the photons nor for the angular divergence of the primary electrons.

(b) The exponentially approximated atomic form factor has been used, $F(g^2)$.

(c) The bremsstrahlung in the field of the electron has not been taken into account.

Now we consider, essentially, the experimental re-

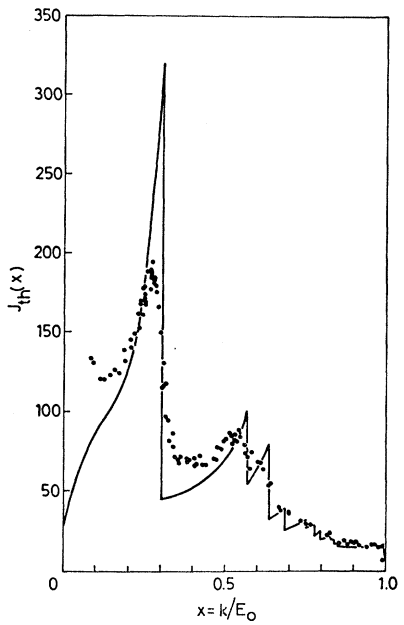

FIG. 19. HEB intensity from diamond crystal, for $\alpha=0$, $\theta=3.44$ mrad, $E_0=4.8$ GeV. Experimental data are compared with theoretical intensity not corrected for experimental resolution. (Desy–Frascati collaboration, Ref. 23.)

sults obtained at Desy[23] by a group of physicists from Desy and Frascati. The Desy synchrotron has an energy of $E_1=6$ GeV, and the angles θ corresponding to the previous ones are $\frac{1}{6}$th of those. But, the relative average $\Delta\theta/\theta$ due to the scattering in the crystal is not larger than in the 1-GeV case if a suitable collimation angle is chosen, as shown before (see also Ref. 22). Good coherent spectra have been obtained at Desy. We present here the following results.[23] In Fig. 19: $E_1=$ 4.8 GeV, $\theta=3.44$ mrad, and the angle $\alpha\equiv(\mathbf{p}_1, \mathbf{b}_1)$ $(\mathbf{b}_1, \mathbf{b}_2)=0$. The angle α is a very important one. In fact while averaging over θ only smoothes the spectrum, averaging over α causes the disintegration of the main peak in many other unresolved peaks. Moreover, for very small x values, i.e., $x\leq 0.05$, if there is a spread in α, other points of the row $b_2=0$ may enter in the

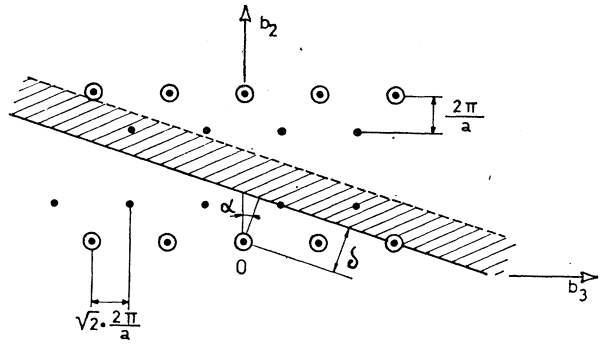

FIG. 20. Intersection of the momentum space with the first reciprocal lattice plane of a diamond crystal for the case at which the HEB spectrum of Fig. 21 was measured (a schematic drawing).

momenta region, causing a new rise in the bremsstrahlung intensity for $x\to 0$.

It has been shown (see Sec. III.A) that the one-point spectrum gives the maximum polarization value available in principle. In Sec. III.C numerical results concerning the choice of a certain crystal orientation are shown. The Desy group[23] showed that this goal is actually reached by choosing a very large angle θ for the crystal, and by rotating the crystal by a small angle α around the $\mathbf{p}_1$ direction. Figure 20 shows the situation in the reciprocal lattice plane chosen by Desy group. Only the point $h_2=0$, $h_3=4$ is effective. Figure 21 shows the experimental results in comparison with the theoretical calculation. The theoretical value

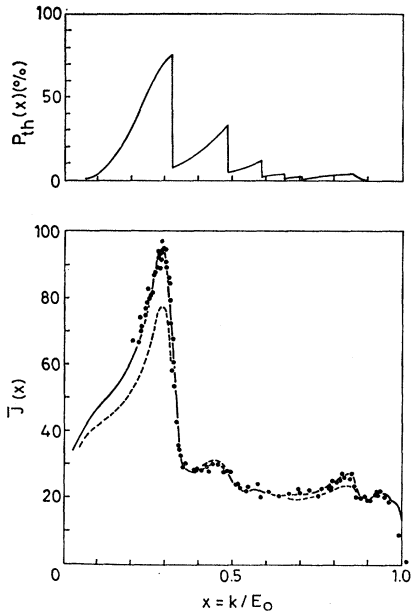

FIG. 21. HEB intensity and polarization from a diamond target. Experimental "one-point" spectrum compared with the averaged intensity and theoretical polarization values; $\alpha=1.5°$, $=50$ mrad, $E_0=4.8$ GeV (——) Hartree potential, (– – –). θ exponential potential. (Desy–Frascati collaboration results, Ref. 23.)

of the polarization is shown at the top. The following remarks are important:

(1) The polarization at the top of the peak has a theoretical value of ~80%.

(2) The θ value is 50 mrad, and $\alpha=26$ mrad. The θ value is larger by a factor of 10 than that of the previous spectrum. This almost gives the certitude that this method would work at much higher energies.

(3) The height of the peak and the polarization value at the top are much more insensitive to a slight accidental misalignment of the crystal than in multipoints peak case.

(4) There is better agreement by using the Hartree atomic form factor.

In 1963 the Frascati group[21] proposed the measurement of polarization of high-energy γ rays by measuring

the electron pair photoproduction in a crystal, now used as analyzer. This group computed the asymmetry ratio $(\sigma_{||}-\sigma_{\perp})/(\sigma_{||}+\sigma_{\perp})=R$, where $\sigma_{||}$ and $\sigma_{\perp}$ denote cross sections with the polarization vector of the incoming photon parallel or perpendicular to the "incident plane" (**K**, **b**), where K is the momentum of the photons and **b** the crystal axis (see Fig. 14).

The "asymmetry ratio" R is an increasing function of the photon energy K. The angles involved in the pair production are larger by a numerical factor than those of the bremsstrahlung. The R value is too small at $E\leq 1$ GeV, and it is higher at $E_1>1$ GeV; for example, $R\geq 20\%$ at 3 GeV. Below 1 GeV the polarization of the Frascati coherent beam has been measured by angular analysis of the electron pair production in an amorphous target by the Frascati group.[20] The Desy group successfully carried out the measurement of the 2-GeV photon peak from 6-GeV bremsstrahlung from a diamond crystal by the analyzing crystal method. They used as an analyzer a second diamond crystal inside the vacuum chamber of a pair spectrometer. They observed the number $N_{\perp}$ of detected symmetrical electron pairs with the photon polarization vector $\boldsymbol{\varepsilon}$ perpendicular to the reference plane. Then they observed the counting rate $N_{||}$ after a rotation of the analyzer diamond by 90°. The polarization values $P=(1/R)[(N_{\perp}-N_{||})/(N_{\perp}+N_{||})]$ obtained are shown in Fig. 22 together the theoretical expected values and the spectrum of the incident photon beam. Good agreement is found. Also here a "single 1-point" asymmetry ratio R has been used. This experimental method

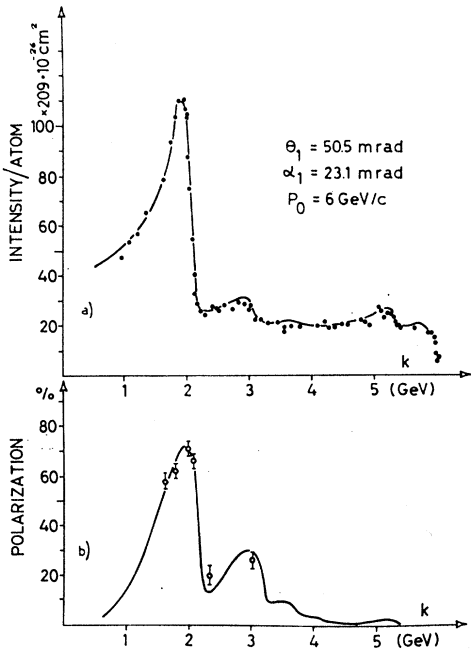

FIG. 22. Measurement of the polarization of the coherent HEB by the analyzing crystal method. (a) "One-point" spectrum obtained with $\theta=50.5$ mrad, $\alpha=23.1$ mrad, $E_0=6$ GeV. (b) Results of the polarization measurements along the former spectrum. (Desy results, see Ref. 24.)

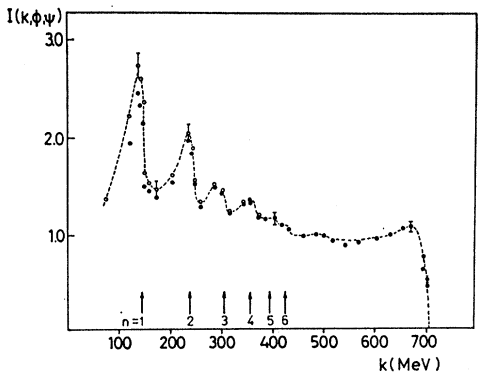

FIG. 23. Intensity of the HEB in a silicon single crystal; $\theta=15.6$ mrad, $\alpha=0$, $E_0=720$ MeV. The circles are the experimental points corrected for vertical losses of the counters. (Tokyo results, see Ref. 25.)

has the important experimental advantage of avoiding any difficult angular selection.

Coherent bremsstrahlung from a silicon single crystal has been extensively studied[25,26] by a collaboration of 10 physicists at the Tokyo 720-MeV electron–synchrotron. They obtained spectra in agreement with the theoretical calculation in which an experimental form factor has been introduced (Fig. 23).

V. CONCLUDING REMARKS

A. Topics Omitted

First we refer to a number of informative theoretical papers of Cabibbo and co-workers,[28] according to which a polarized HEB could be produced by using very thick crystals. The authors show that HEB with linear or circular polarization could be obtained by using crystals of suitable thickness.

Another topic concerns the production of very narrow peaks of coherent HEB by using very thin crystals.[30,31,32] Eventually the problem of measuring the polarization of the HEB calls for a more extensive treatment. In fact these topics, mainly the first two, can best be treated in a survey concerning a more specific comparison between the different methods for producing monochromatic and (or) polarized γ-ray beams, in order to use them in photoreaction experiments. Such a survey may be found in Refs. 33 and 34.

ACKNOWLEDGMENTS

The author would like to express his gratefulness to Professor E. Amaldi; in fact this paper would never have been finished without his constant and stimulating interest. Thanks are due to Dr. G. Sette for reading the manuscript.

[30] J. De Wire and F. R. Mozley, Nuovo Cimento **27**, 1281 (1963).
[31] G. Lutz, Desy Rept. 66/37, Nov. 1966.
[32] G. Bologna, Nuovo Cimento **49A**, 756 (1967).
[33] G. Diambrini Palazzi, Proc. Intern. Conf. Electromagnetic Interactions, Dubna (USSR), 1967.
[34] G. Diambrini Palazzi, Proc. Conf. Electron-Photon Interactions, Stanford, Calif., 1967 (to be published).